Seifert Surfaces of Maximal Euler Characteristic

Rasmus Hedegaard

Department of Mathematical Sciences
University of Copenhagen

MASTER THESIS
Submitted *25th March, 2010*

Supervisor: Nathalie Wahl
Department of Mathematical Sciences
University of Copenhagen

Foreword.

Given a link $L \subset S^3$, a Seifert surface S for L is a compact, orientable surface with boundary L. The Euler characteristic $\chi(L)$ of the link L is defined to be the maximum over all Euler characteristics $\chi(S)$ of Seifert surfaces S for L. Seifert surfaces exist for all L, and this definition presents itself with the problem of calculating $\chi(L)$. An easily applicable method for producing Seifert surfaces is known as Seifert's algorithm. For a given link L, this algorithm takes as input a diagram D for L and returns a Seifert surface for L. The output of the algorithm generally depends on the choice of diagram, and as such, we define the canonical Euler characteristic $\chi_c(L)$ of a link L to be the maximum over all Euler characteristics $\chi(S)$, where S is now a Seifert surfaces for L produced by Seifert's algorithm. It is thus true that for all links L, we have $\chi(L) \geq \chi_c(L)$. It will be seen to be straightforward to calculate $\chi(S)$, when S is a surface produced by Seifert's algorithm. Whenever the inequality $\chi(L) \geq \chi_c(L)$ reduces to an equality, we thus have immediate access to finding $\chi(L)$. This thesis considers the question: For which links L do we have equality in $\chi(L) \geq \chi_c(L)$? We show first that we do have equality for the class of links known as the alternating links. Following a completely different path, we prove then that we also have equality for a class of links known as the alternative links (of which alternating links are a special case), and also that the maximal Euler characteristic Seifert surface S is produced by applying Seifert's algorithm to an alternative diagram.

I thank my supervisor Nathalie Wahl for her patience and resiliency in dealing with my many questions, and for her always helpful insights.

Forord.

En Seifertflade S for et givet link L er en kompakt, orienterbar flade, som har L som rand. Eulerkarakteristikken $\chi(L)$ af linket L er pr. definition maksimum over alle Eulerkarakteristikker $\chi(S)$, hvor S er en Seifertflade for L. Seifertflader eksisterer for alle L, og denne definition giver anledning til spørgsmålet om, hvordan $\chi(L)$ beregnes. En letanvendelig metode til at producere Seifertflader er Seiferts algorithme. For et givet link L tager algoritmen et diagram D for L som input, og returnerer en Seifertflade for L. Generelt vil algoritmens output afhænge af diagramvalget, og vi definerer den kanoniske Eulerkarakteristik $\chi_c(L)$ af linket L til at være maksimum over alle Eulerkarakteristikker $\chi(S)$, hvor S er en Seifertflade for L produceret af Seiferts algoritme. Det er således tilfældet for alle links L, at $\chi(L) \geq \chi_c(L)$. Eulerkarakteristikken $\chi(S)$ kan let beregnes, når S fremkommer ved Seiferts algoritme. Således gælder, at når uligheden $\chi(L) \geq \chi_c(L)$ reduceres til en lighed, så har vi umiddelbar adgang til at beregne $\chi(L)$.

Dette speciale beskæftiger sig med spørgsmålet: For hvilke links L har vi lighed i $\chi(L) \geq \chi_c(L)$? Vi viser først at vi har lighed for en klasse af links kaldet de alternerende links. Ved at gå en helt anden vej viser vi herefter, at vi også har lighed for en klasse af links kendt som alternative links (som alternerende links er et specialtilfælde af), og at Seifertfladen S med maksimal Eulerkarakteristik opnås ved at anvende Seiferts algoritme på et alternativt diagram.

Jeg takker min vejleder Nathalie Wahl for hendes vedholdenhed og tålmodighed med mine mange spørgsmål, og for hendes altid brugbare indsigt.

Contents

Chapter 1

Introduction

This chapter takes care of introducing the necessary concepts for us to be able to speak freely on the subject of Seifert surfaces.

1.1 The intersection product on homology

In the upcoming proof that alternating projections give rise to maximal Euler characteristic Seifert surfaces via Seifert's algorithm (all to be defined), we will consider the intersection of certain submanifolds of S^3, and at that point, it will be convenient to know that this intersection is homology invariant. To prepare ourselves, we thus introduce the intersection product on the homology of a manifold. We follow the work of [2, section VI.11].
Let M^n be a compact, oriented, connected manifold, with or without boundary. Let D denote the inverse map of the Poincaré duality isomorphism, so that $D\colon H_i(M, \partial M) \to H^{n-i}(M)$ or $D\colon H_i(M) \to H^{n-i}(M, \partial M)$. In symbols, we have thus for all $a \in H_i(M, \partial M)$ (or all $a \in H_i(M)$) that

$$D(a) \cap [M] = a, \tag{1.1}$$

where $[M]$ denotes the homology class of M.

Definition 1. *The* intersection product $\bullet$ *is defined to be the map* $H_i(M) \otimes H_j(M) \to H_{i+j-n}(M)$ *(or* $H_i(M, \partial M) \otimes H_j(M) \to H_{i+j-n}(M)$*, or* $H_i(M, \partial M) \otimes H_j(M, \partial M) \to H_{i+j-n}(M, \partial M)$ *) given by* $a \bullet b = D^{-1}(D(b) \cup D(a))$ *(notice the reversal in order).*

Let us note a few algebraic properties of the intersection product. Using the well-known cup-cap

relation $(\alpha \cup \beta) \cap \gamma = \alpha \cap (\beta \cap \gamma)$, we have

$$\begin{aligned} a \bullet b &= D^{-1}\left(D(a) \cup D(b)\right) \\ &= (D(b) \cup D(a)) \cap [M] \\ &= D(b) \cap (D(a) \cap [M]) \\ &= D(b) \cap a, \end{aligned}$$

which is useful in algebraic manipulations with the intersection product. The intersection product is commutative in the sense that $a \bullet b = (-1)^{(n-\deg(a))(n-\deg(b))} b \bullet a$, which follows immediately from the identity $D(a \bullet b) = D(b) \cup D(a)$. Furthermore, it is associative, as can be seen from the calculation

$$\begin{aligned} D\left(a \bullet (b \bullet c)\right) &= D(b \bullet c) \cup D(a) \\ &= (D(c) \cup D(b)) \cup D(a) \\ &= D(c) \cup (D(b) \cup D(a)) \\ &= D(c) \cup D(a \bullet b) \\ &= D\left((a \bullet b) \bullet c\right). \end{aligned}$$

We state now the crucial theorem on the intersection product. To prove the theorem, we would have to introduce a bunch of mathematics, none of which will be needed later. The interested reader may instead consult [2].

Theorem 1. *Let W be a manifold with boundary, and let $K, N \subseteq W$ be embedded submanifolds. Assume that K meets ∂W transversely in ∂K, and similarly that N meets ∂W transversely in ∂N. Assume also that $K \pitchfork N$ in W, i.e. that K and N intersect transversely. Then we have*

$$[K \cap N]_W = [N]_W \bullet [K]_W.$$

1.2 Seifert surfaces

Moving up in dimension and looking at surfaces instead of links turns out to be useful in the classification of knots. In particular, we consider the following specific surfaces.

Definition 2. *Given an oriented link $L \subset S^3$, a* Seifert[1] surface *for L is an oriented, compact surface, whose boundary is the link L.*

It is not immediately clear from this definition that Seifert surfaces always exist, but in fact they do, as we show in the next section. It is well-known what the Euler[2] characteristic $\chi(S)$ of a surface S is, and the Euler characteristic of Seifert surfaces for a given link gives rise to the following definition.

[1] Herbert Seifert: 1907 – 1996, Germany
[2] Leonhard Euler: 1707 – 1783, Switzerland

Definition 3. *Let L be a link. By the* Euler characteristic $\chi(L)$ *of L, we mean the quantity*

$$\chi(L) = \max\{\chi(S) | S \text{ is a Seifert surface for } L\},$$

and we say that a Seifert surface S has maximal Euler characteristic, *if $\chi(S) = \chi(L)$.*

Of course our notion of Euler characteristic of a link should not be confused with the usual notion, in which the Euler characteristic of any link is 0. The link Euler characteristic is a link invariant. Indeed, if L_1 and L_2 are equivalent links, then any orientation-preserving homeomorphism $\phi\colon S^3 \to S^3$ maps a maximal Euler characteristic Seifert surface for L_1 to a maximal Euler characteristic Seifert surface for L_2.
For a knot K, it is true that a maximal Euler characteristic Seifert surface for K is the same as a minimal genus Seifert surface for K. Indeed, for a compact, orientable surface S with boundary, we have $\chi(S) = 2C(S) - 2g(S) - n(S)$, where $C(S)$ denotes the number of connected components of S, $g(S)$ denotes the genus of S, and $n(S)$ denotes the number of boundary components of S. If S is a Seifert surface for a knot, we have then $\chi(S) = 2 - 2g(S) - 1$, thus showing that $\chi(S)$ is maximal exactly when $g(S)$ is minimal.

1.3 Seifert's algorithm

Seifert's algorithm is a procedure, which produces Seifert surfaces for links. The algorithm is useful in that it returns a Seifert surface for any given oriented link, in that the algorithm is easily comprehensible and applicable, and in that the resulting Seifert surface is comprised of "basic" geometric pieces, namely discs and bands ($I \times I$'s, where $I = [0, 1]$).
Let L be an oriented link, and let D be a corresponding link diagram, i.e. a diagram obtained by choosing some projection of $L \subset S^3$ onto an $S^2 \subset S^3$. Then the algorithm takes D as input, and the output of the algorithm will very much depend on this choice of diagram. For each crossing of the diagram, we make a change, but only at this crossing, so that the appearance of the link at any other place will remain the same. The change will be made as illustrated in figure 1.1.

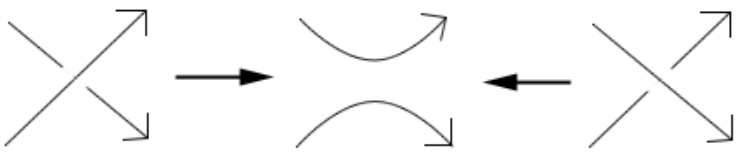

Figure 1.1: Changing the link at each crossing.

This gives rise to a disjoint collection of circles, which we refer to as *Seifert circles* (or sometimes Seifert circuits). If one circle is inside (or outside) of another circle, these two circles are said to be *nested* Seifert circles. If necessary, we lift some of the Seifert circles, such that nested Seifert circles

are positioned at different heights in space. Each Seifert circle bounds a disc, and each of these discs can now be taken to be disjoint. For each crossing of D, we position a band with a half twist between the relevant pair of discs, taking care to twist it in the direction matching the nature of the corresponding to crossing. This surface does indeed have L as boundary. Furthermore, it is compact and orientable, the latter of which may not be apparent from the algorithm, but which has been checked in [6], in which can also be found a more detailed account of Seifert's algorithm.
As an example, we apply Seifert's algorithm to the so-called "Stevedore's Knot", which is a prime knot of 6 crossings, also known as 6_1 in the knot tables, see figure 1.2.

Figure 1.2: Stevedore's knot, or the knot 6_1.

Give the knot some orientation. For knots, the surface obtained by Seifert's algorithm is – as a set – independent of the orientation of the knot diagram, while for links, the output differs for different orientations. In figure 1.3, we see the oriented Stevedore knot, and the corresponding set of Seifert circles.

Figure 1.3: Constructing the Seifert circles from a diagram of the Stevedore knot.

We have a pair of nested circles, which we regard to be at different heights of space. For each circle, fill in a disc, so that the surface thus far consists of five disjoint discs. The next step is to connect the various discs by twisted bands, one for each crossing of the Stevedore knot diagram. The resulting surface is shown in figure 1.4, and it has the knot as its boundary.

Figure 1.4: The result of applying Seifert's algorithm to the given diagram of Stevedore's knot.

Now, the main question of this thesis is the following. When given a diagram of a link L, Seifert's algorithm does produce a Seifert surface for L, but there is no reason why this Seifert surface should have maximal Euler characteristic. One could then hope that for a given link, the link has *some* diagram, for which Seifert's algorithm produces a maximal Euler characteristic surface, but this turns out to be too much to hope for. The question is then, which links have a diagram for which the Seifert algorithm *does* produce a maximal Euler characteristic Seifert surface. We prove that the classes of alternating and alternative links (to be defined later) have this property.
Given a link L, we define the canonical Euler characteristic $\chi_c(L)$ as follows:

$$\chi_c(L) = \max\{\chi(S) | S \text{ is a Seifert surface for } L \text{ produced by Seifert's algorithm}\},$$

where $\chi(S)$ denotes the Euler characteristic of the surface S. We certainly have $\chi(L) \geq \chi_c(L)$ for all L, and our main question is this: For which L do we have equality?

Chapter 2

Alternating links

We give here a proof that for an alternating link L, the canonical Euler characteristic of L coincides with the Euler characteristic of L. The proof follows [4], but compared to that work, details have been supplied. Let us first define alternating links.

Definition 4. *Given a link $L \subset S^3$, and a diagram $D \subset S^2$ for L, the diagram D is said to be* alternating*, if for each component of the link, the crossings alternate under, over, under, over, etc. as you traverse the component. A link is said to be alternating, if it has an alternating diagram.*

A link being alternating thus refers to a particular property of a particular diagram of the link. However, in the words of R.H. Fox: "What *is* an alternating knot?", in which he asks for a topological characterization without mention of diagrams. Such a characterization is as yet unknown. Despite this, alternating links are known to have lots of interesting properties, including the one we are momentarily going to prove. For other properties, see [9, chapters 4 and 5] and [1].

The following lemma is general in the sense that it does not assume that the link in question has an alternating projection.

Lemma 1. *Let $L \subset S^3$ be a link, and let S be a Seifert surface for L, which is not of maximal Euler characteristic. Then there exists a Seifert surface T for L, such that $\chi(T) > \chi(S)$, and such that $\mathring{S} \cap \mathring{T} = \emptyset$, i.e. such that T and S do not intersect except for at their common boundary.*

Proof. Choose first a Seifert surface T for L, such that $\chi(T) > \chi(S)$. This is possible, as S is not of maximal Euler characteristic. Let $N(L)$ denote a tubular neighborhood of L, chosen so small that both S and T intersect each meridian of $N(L)$ just once. We show first that S and T then represent the same homology class in the homology group $H_2(S^3 - \mathring{N(L)}, \partial N(L))$, so that $[S] = [T]$. First, notice that we have a group isomorphism $H_2(S^3 - \mathring{N(L)}, \partial N(L)) \simeq H_2(S^3, \overline{N(L)})$, whence it suffices to show that $[S] = [T]$ in the latter group. We have the following portion of the long exact sequence in homology:

$$\cdots \to H_2(S^3) \to H_2(S^3, \overline{N(L)}) \to H_1(\overline{N(L)}) \to H_1(S^3) \to \cdots,$$

and as $H_1(S^3) = H_2(S^3) = 0$, the sequences reduces to

$$0 \to H_2(S^3, \overline{N(L)}) \to H_1(\overline{N(L)}) \to 0,$$

so that we have an isomorphism $H_2(S^3, \overline{N(L)}) \to H_1(\overline{N(L)})$. But the group $H_1(\overline{N(L)})$ is generated by a longitudinal line going once around the torus $N(L)$, and thus an element of this group is determined by the number of times it intersects a meridional disc of $\overline{N(L)}$. Correspondingly, a member of $H_2(S^3, \overline{N(L)})$ is determined by the intersection number with meridians of $\overline{N(L)}$, but the tubular neighborhood was so constructed to make sure that S and T intersected each meridian of $\partial N(L)$ just once, whereas $[S] = [T]$.

Consider now the long exact sequence in homology for the pair $(S^3 - \mathring{N(L)}, \partial N(L))$, or rather the following rather small portion of it:

$$H_2(S^3 - \mathring{N(L)}, \partial N(L)) \to H_1(\partial N(L)),$$

where the map is, of course, a boundary map ∂. Knowing that $[S] = [T]$ in the left-hand group implies that $[\partial S] = \partial([S]) = \partial([T]) = [\partial T]$, so that the boundaries of S and T represent the same homology class on the torus $\partial N(L)$, whence we can isotope S and T to have no intersection on the boundary $\partial N(L)$. Consequently, we can also isotope S and T to have no intersection inside of $N(L)$, except for at the link L. Outside of $N(L)$, the surfaces S and T may then be put in general position so that $(S \cap T) - N(L)$ consists of a finite number of simple closed curves: There are no arcs in $S \cap T$, as S and T have no common point on $N(L)$.

From now on, whenever we speak of S and T, we think of them in the complement $S^3 - N(L)$, so that $S \cap T$ is the finite union of simple closed curves, as described.

Choose a point $x \in S^3 - (N(L) \cup S \cup T)$, and define the map

$$\phi_x \colon S^3 - (N(L) \cup S \cup T) \to \mathbb{Z}$$

by

$$\phi_x(t) = \langle \lambda, S \rangle - \langle \lambda, T \rangle,$$

where λ is any oriented path from x to t, and where $\langle . \, , . \rangle$ denotes the algebraic intersection number. We argue that this is well-defined. Let λ and λ' be two oriented paths from x to t, so that $\lambda \cup (-\lambda')$ is a simple closed curve. As S and T represent the same homology class, we know from the theory of intersection products that

$$\langle \lambda \cup (-\lambda'), S \rangle = \langle \lambda \cup (-\lambda'), T \rangle.$$

By definition we have

$$\langle \lambda \cup (-\lambda'), S \rangle = \langle \lambda, S \rangle - \langle \lambda', S \rangle,$$
$$\langle \lambda \cup (-\lambda'), T \rangle = \langle \lambda, T \rangle - \langle \lambda', T \rangle,$$

and by rearranging, we see that ϕ_x is independent of the path chosen from x to t. We argue now that we may choose an x, such that the map ϕ_x is always non-negative, i.e. $\phi_x(t) \geq 0$ for all $t \in S^3 - (N(L) \cup S \cup T)$: Suppose contrariwise that there are no points x for which ϕ_x is non-negative. As S and T are in general position, the complement $S^3 - (N(L) \cup S \cup T)$ consists of a

finite number of path-components $J_1, J_2, \ldots, J_n$. If x and t are points in the same path-component, then certainly $\phi_x(t) = 0$. Choose n point $x_1, \ldots, x_n$, such that $x_i \in J_i$ for all $i \in \{1, 2, \ldots, n\}$. The contrary assumption thus amounts to the statement that for all x_i, there is an x_j, such that $\phi_{x_i}(x_j) < 0$. Starting with x_1, there is a path to some x_j, such that $\phi_{x_1}(x_j) < 0$. After a possible renaming of indices, assume that $x_j = x_2$. For x_2, there is another path to another x_j, such that $\phi_{x_2}(x_j) < 0$, say $x_j = x_3$. Continue this process. As there are only finitely many x_j, we reach at some point an x_k, such that the point x_j with $\phi_{x_k}(x_j) < 0$ is a point we have already encountered, i.e. $x_j = x_r$ for some $r \in \{1, 2, \ldots, k-1\}$. But then the composition of the paths from x_r to x_{r+1} to x_{r+2} to $\cdots$ to x_k to x_r is a path from x_r to itself such that $\phi_{x_r}(x_r) < 0$, an obvious contradiction. In fact, if $S \cap T \neq \emptyset$, we may choose an x such that $\max \phi_x \geq 2$. Indeed, consider some intersection circle λ of $S \cap T$. In a small tubular neighborhood of this intersection, the surface S is just a cylinder, and likewise for T. Locally, the intersection has the appearance as that of figure 2.1.

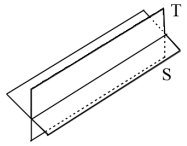

Figure 2.1: Locally, the intersection of S and T divides the surrounding space into four regions.

Locally, the surfaces S and T thus give rise to four regions $R_1, \ldots, R_4$, which may or may not be distinct. By symmetry, we may assume that the surfaces are oriented as shown in figure 2.2, where the orientation on T is the negative orientation of the given one. But in this picture, we may choose as our x a point in the lower left region, and as our t, we may choose a point in the upper right region. We see that for these choices, we can choose a path from x to t that pass through surfaces twice in the positive direction, and we have then $\phi_x(t) = 2$. Hence $\max \phi_x \geq 2$.

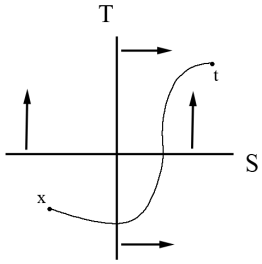

Figure 2.2: Finding points x and t, such that $\phi_x(t) = 2$.

Now, let J be a region that maximizes ϕ_x. We have two cases. In the first case, we change the surface T to obtain another surface T', and in the second case we change S to obtain another surface

T'. In detail:

$$\text{If } \chi(\overline{J} \cap S) \geq \chi(\overline{J} \cap T), \quad \text{let } T' = (T - (\overline{J} \cap T)) \cup (\bar{J} \cap S), \tag{2.1}$$

$$\text{If } \chi(\overline{J} \cap S) < \chi(\overline{J} \cap T), \quad \text{let } T' = (S - (\overline{J} \cap S)) \cup (\bar{J} \cap T). \tag{2.2}$$

In any case, perform a tiny isotopy on the new surface T' to assure that T' and S are again in general position. Let us check what happens near the region J. Before doing surgery as described above, the local situation near the region J is as pictured in figure 2.3. In this figure, the region J must be positioned in the lower left corner. Otherwise one could pass through surfaces in the positive direction a lesser number of times than if J had indeed been to the lower left, contradicting that J is a region maximizing ϕ_x. For a similar reason, the path that gives rise to this maximum must pass through the upper right region.

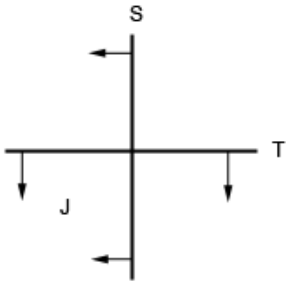

Figure 2.3: A region J, which maximizes the map ϕ.

If we have the case that $\chi(\overline{J} \cap S) \geq \chi(\overline{J} \cap T)$, then we replace whatever part of T in $\overline{J}$ by a copy of the part of S in $\overline{J}$, and similarly for the other case. In terms of figure 2.3, the two cases are as pictured in figure 2.4.

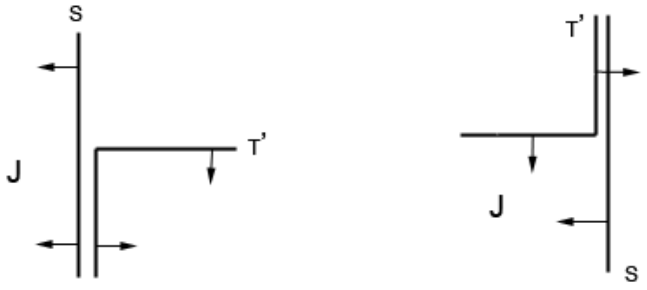

Figure 2.4: Left: Replacing $\overline{J} \cap T$ by $\overline{J} \cap S$. Right: Replacing $\overline{J} \cap S$ by $\overline{J} \cap T$.

Certainly T' still satisfies $\chi(T') > \chi(S)$, because T' was constructed by removing part of a surface, and by letting a part of no less Euler characteristic take its place. The crucial point is that the value

of ϕ_x at a point of J has been lowered by one. Indeed, whichever of the two cases of figure 2.4 we are in, we pass through one less surface to reach J. Define the map $\phi_1 \colon (N(L) \cup S \cup T') \to \mathbb{Z}$ as we defined ϕ above, but with the surface T' taking the place of T, and where we have chosen an x such that $\max \phi_1 \geq 2$ (or such that $\phi_1 \geq 0$ in case $S \cap T' = \emptyset$). By the above argument, we have that either $\max \phi_1 < \max \phi$, or that $\max \phi_1 = \max \phi$, but where the number of regions where ϕ_1 is maximal is less than the number of regions where ϕ is maximal. It follows inductively that after a finite number of iterations we obtain the required Seifert surface. □

The proof above differs from the proof in [4] in the following way. In [4], before making the surgeries of (2.1) and (2.2), the author argues that we may assume that no component of $S \cap T$ bounds a disc in neither S nor T. This seems unnecessary, as we do not appear to make use of it in the above proof. This lemma combined with induction is the essence of proving the desired theorem.

Theorem 2. *Let $L \subseteq S^3$ be an oriented link, and let S be the surface obtained from Seifert's algorithm by applying it to an alternating projection of L. Then S is a maximal Euler characteristic Seifert surface.*

Proof. Suppose S is not connected. Then each connected component of S consists of a collection of discs with twisted bands between some of them. If S_1 is one such connected component, we can then find a 2-sphere Q separating S_1 from the rest of S. We agree that the side of Q containing S_1 is the inside of Q. Inside of Q, we then have a part L_1 of the entire link L. The surface S_1 is a Seifert surface in its own right, and it is in fact the Seifert surface obtained from Seifert's algorithm by restricting the projection of L to the relevant link component(s) L_1. Suppose R is a maximal Euler characteristic Seifert surface for L. Then if R passes through the 2-sphere Q, we can perform surgery on R, in which we replace a cylinder by two discs, thus making R disjoint from Q, see figure 2.5.

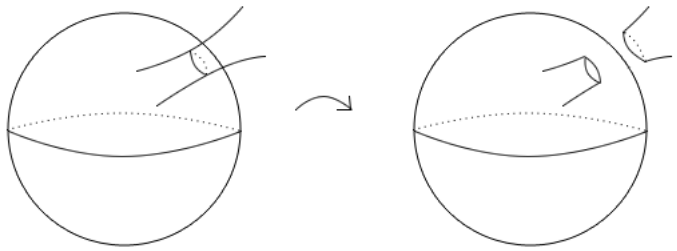

Figure 2.5: Performing surgery to make R disjoint from Q.

After the surgery, if any part of R outside of Q is closed, throw it away. The result is still a Seifert surface for L. On the other hand, if the surgery gives rise to a non-closed component of R outside of Q, then the Euler characteristic of this new Seifert surface is strictly larger than that of R, contradicting that R has maximal Euler characteristic. In conclusion, any maximal Euler characteristic

Seifert surface may be assumed to have one component completely contained inside of Q, and the other part completely contained in the outside of Q. Then S is a maximal Euler characteristic Seifert surface for L, if and only if S_1 is a maximal Euler characteristic surface for L_1, and $S - S_1$ is a maximal Euler characteristic Seifert surface for $\partial(S - S_1)$. Iterating this argument, we see that we may assume that S is connected.

We prove the theorem by induction. A link with a projection of 0 crossings has as its diagram a disjoint union of circles. Seifert's algorithm applied to such a diagram gives a disjoint collection of discs, which is certainly the maximal Euler characteristic Seifert surface for this link. Assume now that the theorem is true for all links with alternating projections of at most n crossings, and let an alternating projection of $n+1$ crossings for a link L be given. The proof proceeds by considering two cases for the Seifert surface S obtained from Seifert's algorithm. Remember that we may assume that S is connected.

Case 1. All Seifert circles are unnested.

Obtain a graph from S as follows. The surface S is composed of discs and twisted bands. On each disc of S, position a vertex. For each pair of discs with a twisted band between them, draw an edge between the corresponding vertices, and call the graph so obtained G_S. Suppose first that G_S has no cycles, i.e. that G_S is a tree. Then S has the appearance such as that of figure 2.6.

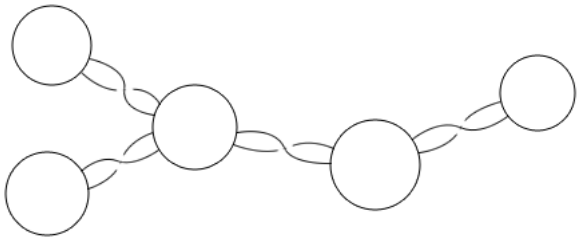

Figure 2.6: A Seifert surface S for which G_S is a tree.

Any such Seifert surface S has the homotopy type of a point, whereas its Euler characteristic is 1. So certainly it is a maximal Euler characteristic Seifert surface. It remains to consider the case, where G_S does contain a cycle, such as that of figure 2.7.

Figure 2.7: Part of the result of Seifert's algorithm, when G_S does contain a cycle.

Since the circles of S are unnested, we can isotope S to lie in some $S^2 \subset S^3$, except for small neighborhoods of the crossings. Recall that L had a diagram of $n+1$ crossings. Pertube the link L slightly, so that it only intersects S^2 in a finite number of points - in particular, for each crossing (corresponding to a twisted band of the Seifert surface), we take care that there are four intersections as shown in the left-hand-picture of figure 2.8, but also such that each such intersection is shared by two crossings, as in the right-hand-picture of the same figure. As L has $n+1$ crossings, as L intersects S^2 four times for each crossing, and as each intersection is shared by two crossings, the total number of points in $L \cap S^2$ is $4(n+1)/2 = 2n+2 = 2(n+1)$.

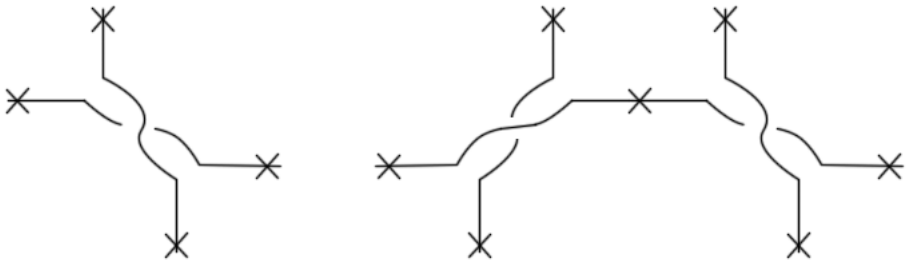

Figure 2.8: The link L intersects S^2 four times at each crossing.

With this choice of intersections, figure 2.7 takes on the appearance of figure 2.9, in which dotted lines represent part of the link which are *below* S^2, and where unbroken lines represent parts of the link which are *above* S^2. As before, intersections between L and S^2 are denoted by X's in the drawing.

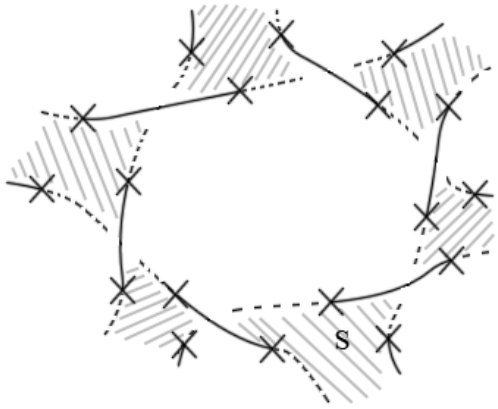

Figure 2.9: Setting up the link to intersect S^2 in the pattern shown.

Notice how we utilize the alternating property of the diagram: Had a strand passed two consecutive crossings by going over, we could not have made the same construction. In figure 2.10, we draw in pitch-black the part of the surface S in S^2, i.e. the part drawn in black is $S \cap S^2$, so that S is entirely positioned in S^2, except for at the boundary $\partial S = L$, which has been lifted or lowered slightly at various places.

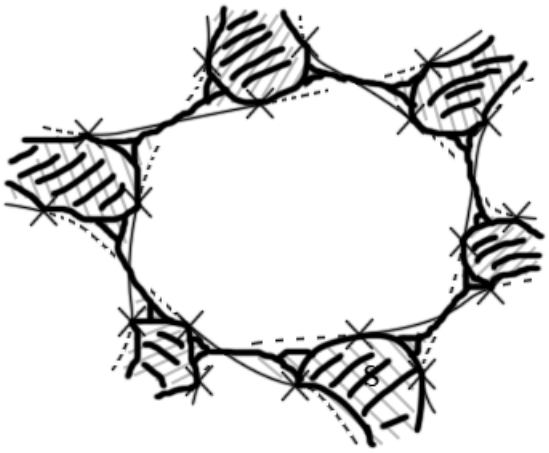

Figure 2.10: In pitch-black: $S \cap S^2$.

Notice that in this figure $S \cap S^2$ encapsulates a disc D; D is a disc in the complement $S^2 - S$, whose boundary contains some of the intersection points of $L \cap S^2$ (in our particular drawing, it contains six such points).

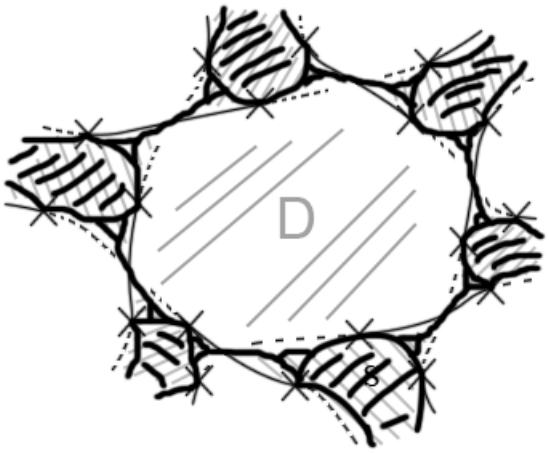

Figure 2.11: The disc D contains some of the points of $L \cap S^2$.

In fact, we argue that $\partial D \cap L$ can consist only of an *even* number of points. Each Seifert circle has some orientation. In the left-hand-side of figure 2.12, one Seifert circle has been given an orientation. In the right-hand-side picture, we see how this orientation is transferred to the adjacent Seifert circle through the twisted band. Notice that the orientation on this adjacent Seifert circle is clockwise, opposite the counterclockwise orientation of its neighbor. For the cycle of discs in figure 2.7 to be part of an orientable surface, we must thus have an even amount of Seifert circles in the cycle. In conclusion, we have that $\partial D \cap L$ consists of $2k$ points for some positive integer k.

Figure 2.12: Orientations reverse from circle to circle.

Assume now that S is not a maximal Euler characteristic Seifert surface, and let T be a Seifert surface as in lemma 1, so that $\mathring{S} \cap \mathring{T} = \emptyset$, and $\chi(T) > \chi(S)$. After a small isotopy, we may assume that T and S^2 have transversal intersection. As $S^2 \cap L$ consists of an even number of points, namely $2(n+1)$, then since T has L as its boundary, the intersection $T \cap S^2$ consists of $n+1$ arcs and some finite set of simple closed curves. For any circle C of $T \cap S^2$, we perform surgery on T, replacing a small cylinder $S^1 \times D^1$ around C by two discs $S^0 \times D^2$, similarly to what happened in figure 2.5. As usual, we throw away all closed components. Doing this for all circles in $T \cap S^2$, we obtain a new

surface T that intersects S^2 only in $n+1$ arcs. Then the new T is a Seifert surface for L, and we have not decreased its Euler characteristic.
The disc $\overline{D}$ has $2k$ points in common with L, as shown in figure 2.11. Take one of the points of $\partial D \cap L$, say P, and take the arc β of $T \cap S^2$ having P as one of its endpoints. Recalling that the heavy black part of figure 2.11 is $S \cap S^2$, and recalling that $\mathring{S} \cap \mathring{T} = \emptyset$, we see that the other end-point of β must also be on ∂D, as β would have to pass through S to access other points. Thus $\overline{D} \cap T$ consists of k arcs.

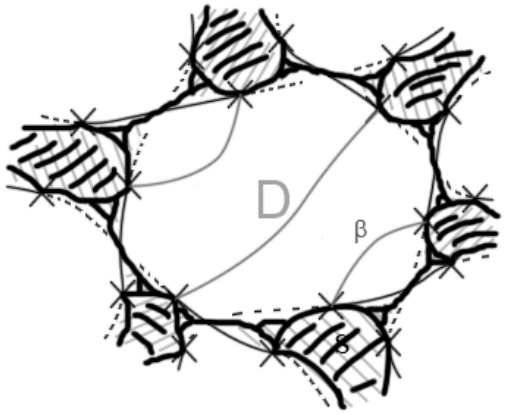

Figure 2.13: The k arcs of $\overline{D} \cap T$.

At least one of the k arcs in $T \cap \overline{D}$ must be an arc between neighboring points of $L \cap \overline{D}$. Take such an arc β, shown in figure 2.13. Also, choose an arc α in $S \cap \overline{D}$ between the same two points, so that α is an arc along the pitch-black part in $\overline{D}$. As α and β are arcs between the same pair of points, we say that α and β are parallel.

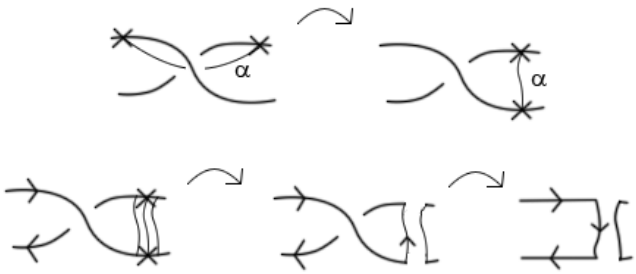

Figure 2.14: Cutting S open along α, and undoing the trivial crossing.

We cut S open along the arc α. It is easier to see the effect of the cutting, if we isotope α to be on one side of the crossing, as shown in the upper part of figure 2.14. In the lower part, we see the effect of cutting S open along α - we undo the trivial crossing so obtained. The resulting surface S' is a

surface of one less crossing than S, and it is the surface obtained by applying Seifert's algorithm to the link $L' = \partial S'$ of n crossings obtained from L by removing the crossing in question. The link L' is certainly also alternating. Similarly, cut open T along the arc β to obtain a Seifert surface T' for L' with $\chi(T') > \chi(S')$. But this contradicts the induction hypothesis that S' was a maximal Euler characteristic Seifert surface.

Case 2. There is a pair of nested Seifert circles.

Take a pair of nested Seifert circles with twisted bands between them, as shown in the upper left corner of figure 2.15. Disregarding the twisted bands, the two discs span a cylinder, as pictured in grey in the upper right picture. This cylinder is of course just a copy of S^2. We declare that the inside of the cylinder S^2 is what appears to be the inside in our figure. As in the previous case, we pertube the link slightly. In the lower left picture, the part of the link in black is outside of the cylinder, while the part of the link drawn with a dotted line is inside the cylinder. Again we make sure that we have four crossings for each twisted band, meaning that if k denotes the number of twisted bands between the two discs (a number, which need not be even), we have $2k$ intersection points in $L \cap S^2$. Again, this construction is possible, as the link projection is alternating. Finally, in the lower right picture, we see in dark grey the part of S still being in S^2. Notice in particular that part of $S \cap S^2$ runs along the twisted bands connecting the discs.

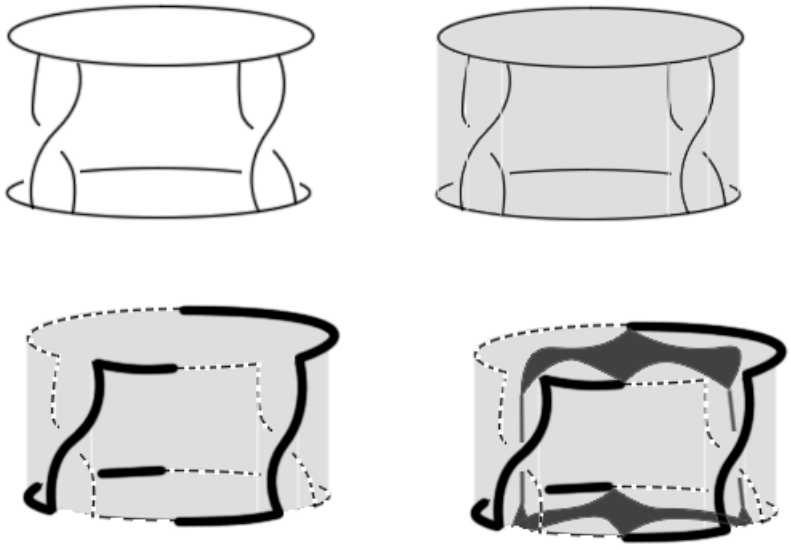

Figure 2.15: A pair of nested Seifert circles, and the corresponding perturbation of the link L.

The rest of the proof goes almost exactly as before. Assume that S is not of maximal Euler characteristic, and take a Seifert surface T, such that $\mathring{S} \cap \mathring{T} = \emptyset$, and assume that T meets S^2 transversely.

Using surgery, we may assume that no component of $T \cap S^2$ is a disc. As $L = \partial T$ has $2k$ points in common with S^2, the set $T \cap S^2$ then consists of k arcs. But such an arc starting from a point on the lower disc must end at the point directly above on the upper disc, since S blocks access to all other points on the sphere. So take any such arc β, as shown in figure 2.16. This arc is parallel to an arc α in $S \cap S^2$. As the two intersection points that are the end-points of α and β are on different strands of the link L, we can cut open the surface S along α and undo a trivial crossing, and so on as in the last part of the previous proof.

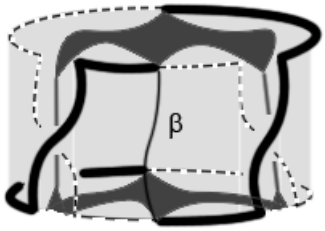

Figure 2.16: The arc β in $T \cap S^2$.

A few details deserves mention. In our drawings, we considered only the twisted bands between the given pair of discs. It may very well be so that there are more twisted bands emanating from the boundaries of these discs, but with other discs as their destinations. Take one such twisted band, and assume it is attached to the top disc. Whichever line segment it is attached to, we may isotope it to be positioned at the part of the link drawn in black, so that it adds no intersection points to the $2k$ points we already have. Notice also that such an extra twisted band does not change the alternating pattern of the twisted bands between the given pair of discs, so that we can still carry out the construction of figure 2.15.

□

Chapter 3

Alternative links

In his paper [7] and in his book [8], Kauffman[1] defines a class of links dubbed *alternative links*. This is a much broader class of links than that of the alternating links, and Kauffman shows that this broader class of links also has the property that any link in the class has a diagram for which the Seifert algorithm produces a maximal Euler characteristic Seifert surface. The definition of alternative links is highly combinatorial, but nevertheless, the end-product will, surprisingly, be the sought-for topological result. In this chapter, we follow primarily the two works of Kauffman. Before reaching the essence of this chapter, namely proving that alternative links have the desired property, we have some combinatorial ground to cover.

3.1 Universes, states, and Jordan trails

In all of this chapter, universes will be the underlying structures on which we do combinatorics.

Definition 5. *A* universe *is a connected, planar, directed (multi-)graph with the property that every vertex has four edges incident to it. An* oriented universe *is a universe such that at each vertex, the adjacent edges have orientations as shown in figure 3.1.*

The "multi" part of the definition of a universe refers to the allowance of multiple edges between the same pair of vertices, and of loops. It will be convenient also to regard a simple closed curve (with no vertices) as a universe.

[1] Louis H. Kauffman: 1945– , USA

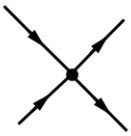

Figure 3.1: The setup at every 4-valent vertex of an oriented universe.

At each vertex, we can draw a black quarter-of-a-disc called a *state marker*, as in figure 3.2.

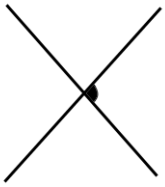

Figure 3.2: A state marker.

The state marker could just as well have been positioned to the north, west or south (from our perspective). By a *region* of a universe, we mean one of the regions into which the universe separates S^2.

Definition 6. *A* state *of a universe is an assignment of one state marker per vertex such that each region contains at most one state marker.*

When drawing a state of a universe U, we let stars occupy regions containing no state markers. An example is the universe shown in figure 3.3, which has four vertices, and in which we have two regions unoccupied by states. Notice also that there are a total of six regions.

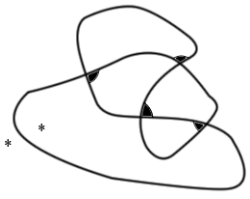

Figure 3.3: A state of a universe.

Given some arbitrary universe, it is not immediately obvious whether or not is has states. Before turning to this question, let us first remark that it was no coincidence in the example above that we had exactly two regions occupied by stars. In fact, the following result goes back to Euler.

Proposition 1 (Euler)**.** *Let U be a universe, let R be the number of regions of U, and let V be the number of vertices of U. Then*

$$R = V + 2.$$

Proof. Each vertex has the form shown in figure 3.4, and may be split in one of the two ways shown in figure 3.5.

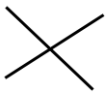

Figure 3.4: A vertex of a universe.

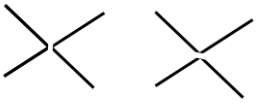

Figure 3.5: The two ways of splitting a vertex.

We claim that at each vertex, one of the two ways of splitting the vertex will result in a connected graph. Indeed, suppose contrariwise that v is the first vertex (in some arbitrary order) of U for which both choices of splittings result in a disconnected graph, and choose one of these splittings. Then the graph has the appearance of figure 3.6, where G_1 and G_2 are connected graphs (since v was chosen to be first with the unpleasant property). The cusps at the splitting are only there for visual aid, and is *not* to be mistaken for vertices.

Figure 3.6: A splitting.

Had we chosen the other splitting at v, the graph would instead have had the appearance of figure 3.7, but as both G_1 and G_2 are connected, it is now possible to travel from any vertex of G_1 to any vertex of G_2, contrary to the assumption that the second splitting gave rise to a disconnected graph.

Figure 3.7: The other splitting.

Splitting a vertex while maintaining connectivity reduces both the number of vertices and the number of regions by one, thus leaving invariant the difference $R - V$. Repeating the procedure of splitting

vertices until none are left leaves us with a simple closed curve of no vertices and (by the Jordan curve theorem) with two regions, thus proving the theorem. □

The result of splitting a crossing will be referred to as a *site*. Thus, the two pictures of figure 3.5 are both sites, again, with the cusps being there for visual aid only, and thus not counting as vertices. By dint of Euler's result, we know that if a universe does have a state, then exactly two regions of the universe will be occupied by stars. We now turn to the problem of existence of states, for whose purpose we study paths in universes, so let P be a path in a universe U, i.e. we may think of P as a succession of edges. Let v be a vertex of U visited by P. If P visits v in the manner shown in the left figure of figure 3.8, then P is said to *cross* the vertex v. If, on the other hand, P proceed across v in the manner of the right figure of figure 3.8, then P is said to *call* v, where the thick line of the figure signifies the path P.

Figure 3.8: The two ways of proceeding across a vertex, crossing and calling.

Definition 7. *A* Jordan[2] trail *on a universe U is a path that traverses the entire universe, using each edge exactly once, and calling every vertex.*

Out of necessity, a Jordan trail will call each vertex exactly twice. A Jordan trail on a universe will become a Jordan curve, if we separate the path at each vertex to form a site, as pictured in figure 3.5; and vice versa, a Jordan curve with sites at the positions of the vertices of a universe corresponds to a Jordan trail by assembling the sites to crossings. It is not yet apparent what Jordan trails have to do with states, but we will see in a moment that Jordan trails exist, if and only if states exist. We have the following auxiliary result.

Lemma 2. *Any universe U admits at least one Jordan trail.*

Proof. The proof of the lemma is very similar to the proof of Euler's result, proposition 1. In that proof, we have already argued that for any given vertex, at least one of the two splittings will leave the graph connected. Pick some order of the vertices, and for each vertex, choose a splitting that retains connectivity. The end result is a simple closed curve with sites at what was before vertices; but such a simple closed curve corresponds to a Jordan trail. □

For an example of applying the method of the proof, see figure 3.9, in which we split the vertices starting from the southmost vertex and continuing in a counter-clockwise fashion. The bottom diagram of that figure is the resulting Jordan curve, whose sites may be resembled to form the corresponding Jordan trail. We promised earlier that states exist, if and only if Jordan trails exist.

[2]Marie Camille Jordan (a guy): 1838 – 1922, France

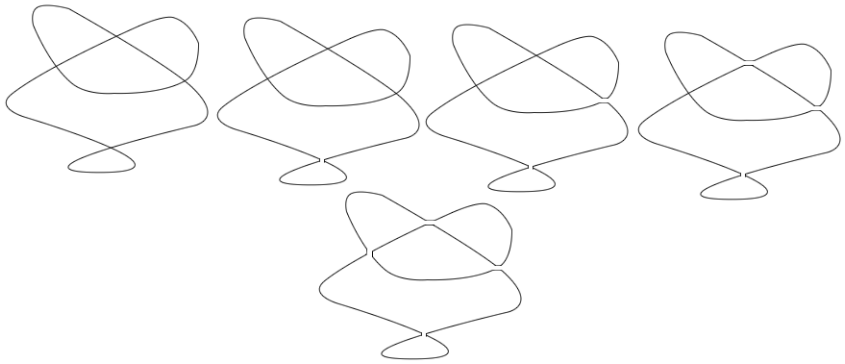

Figure 3.9: Obtaining a Jordan curve with sites from a given universe.

This is an easy corollary to the following more elaborate result, combined with lemma 2.

Theorem 3 (States-trails correspondence)**.** *Let a universe U be given, and choose two adjacent regions of U to occupy stars. Let $\mathcal{S}$ denote the set of all states on U with this choice of fixed adjacent stars, and let $\mathcal{T}$ denote the set of all Jordan trails on U. Then $\mathcal{S}$ and $\mathcal{T}$ are in one-to-one correspondence.*

Proof. First define the map $f\colon \mathcal{S} \to \mathcal{T}$ as follows. Let a state $S \in \mathcal{S}$ be given, and for each vertex of this state, let the state marker at that vertex dictate splitting the crossing according to the rule of figure 3.10.

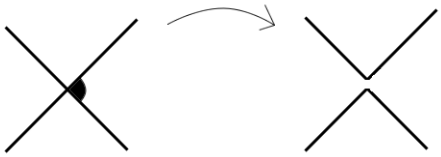

Figure 3.10: A state provides a schema for splitting crossings.

The result of performing this operation for each vertex of U gives rise to a finite set of simple closed curves. We claim that the end result is actually just *one* closed curve, i.e. one Jordan curve, corresponding to a Jordan trail of U. This Jordan trail will be $f(S)$.
To prove this claim, we argue that every time we split a crossing as dictated by the state marker at that crossing, the graph will still be connected. Suppose contrariwise that splitting a certain crossing results in a disconnected graph. We have thus the situation of figure 3.10, where the top graph is not connected to the bottom graph. Call the top graph U_1 and the bottom graph U_2. Then the regions marked 1 and 2 in figure 3.11 was the same region before the splitting took place. Recall that when a crossing is split, the resulting cusps are not to be regarded as vertices, so U_1 and U_2 are universes in their own right.

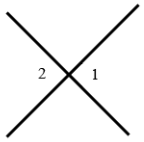

Figure 3.11: Depicting the same crossing as figure 3.10.

Certainly a star cannot occupy region 1 (or 2), because that region had a state marker in it. As the two stars of U occupy adjacent regions, the two stars cannot occupy regions of different U_i, $i = 1, 2$ (since U_1 is separate from U_2). The only remaining possibility is that the two stars occupy adjacent regions of the same U_i, say U_1, implying that there are three regions of U_1 unoccupied by states, contradicting proposition 1. In conclusion, splitting crossings as dictated by the state markers results in a simple closed curve with sites. We can in fact show that the two stars are in distinct regions of this simple closed curve. This can be seen by checkerboard coloring the universe, so that diagonal regions receive the same color, as shown in figure 3.12. When splitting a crossing, only similarly colored regions can become connected, and as the stars are adjacent, they will be in distinct regions of the Jordan curve obtained by splitting crossings.

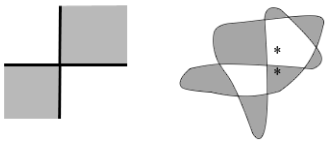

Figure 3.12: Checkerboard coloring a universe.

We define the inverse map $g\colon \mathcal{T} \to \mathcal{S}$ as follows. Let a Jordan trail $T \in \mathcal{T}$ be given. As stars are on different sides of the corresponding Jordan curve J, each point of the complement of J can be reached by a path from a star. Grow two trees in the complement of J, each tree rooted in a star, in such a manner that the tree grows through sites, the tree always branching out to have the necessary number of branches to pass through all sites, and a branch never entering a region which already has a branch in it. At each site, a state marker is placed in the direction of the tree growth, and the site is closed, as pictured in figure 3.13.

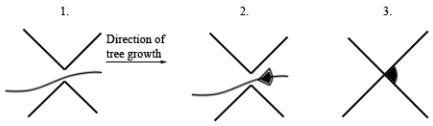

Figure 3.13: Part 1: The tree grows from left to right through the site. Part 2: A state marker is placed in the direction of the growth. Part 3: The site is closed.

The reader may be mystified, in which case figure 3.14 can be considered.

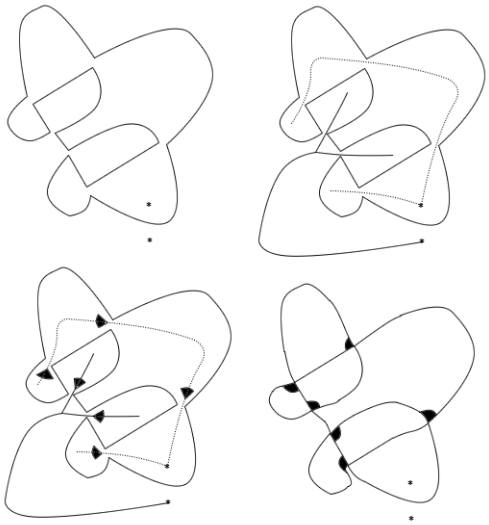

Figure 3.14: Given a Jordan trail, grow trees rooted at the two stars to obtain a state marker at every vertex of U.

One should note that there is no choice involved, when the tree enters a region, i.e. for each region, the tree can only enter that region through one site. This guarantees that the choice of state marker at each vertex is unique, which in turn ensures that $g(T)$ will be well-defined. For the sake of an argument, suppose that the tree could enter a region through two different sites. There are then two different paths from that region to the root (a star), giving rise to a simple curve. But this closed curve then divides the Jordan curve in two, contradicting connectedness. Finally, let us remark that we do in fact obtain a state. Certainly every vertex of U receives a state marker, as the trees grow through all sites of J, and it remains only to see that no region contains more than one state marker. But this is true, since a region receives a state marker as soon as the tree grows into that region, and since the tree does not grow into the same region twice.
It is immediate from the definitions of f and g that $f \circ g$ and $g \circ f$ are both the identity (on their respective sets). Indeed, given a Jordan trail T, the state $g(T)$ is the one whose state markers exactly dictate splitting each vertex as to obtain T, whereas $f \circ g(T) = T$. And given a state S, consider

the Jordan trail $f(S)$, and pick a star. The sites adjacent to this star (that is, the sites first visited by the tree) correspond to the vertices of U bounding the region of the star. Each of these vertices were split according to figure 3.10, and thus the state marker at each of these vertices was on one of the open sides of the corresponding site. But certainly the state markers could not have been at the side of the site containing the star, so the first stage of tree growth does position the first set of state markers correctly. Iterating this argument shows that $g \circ f(S) = S$. □

3.2 The clock theorem

Let U be a universe, and for a fixed choice of adjacent stars, consider a state of U. Suppose that X and Y are two regions of U that share common boundary, such that both regions have a state marker, and such that the state markers are positioned as in the first picture of figure 3.15. Moving each of the two state markers in a clockwise direction, such that the two regions exchange state markers, as shown in the second part of 3.15, is said to be a *clockwise move*. The term *counterclockwise move* is defined analogously, and by a *state transposition*, we mean either a clockwise move or a counterclockwise move.

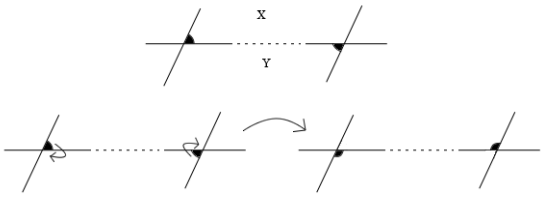

Figure 3.15: Switching two state markers, in a clockwise motion.

Definition 8. *A state of a universe is said to be* clocked*, if it admits no counterclockwise moves, and it is said to be* counterclocked*, if it admits no clockwise moves.*

For an example of a counterclockwise move, see figure 3.16. The picture to the right on this figure is a clocked state, as it admits only clockwise moves.

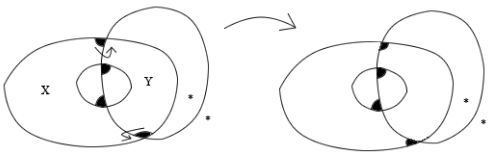

Figure 3.16: A state of a universe for which we make a counterclockwise move.

Recall that a *lattice* is a non-empty partially ordered set $(A, \leq)$, such that any two elements $a, b \in A$ have a least upper bound and a greatest lower bound. The former is usually denoted by $a \vee b$, and

is called the *meet* of a and b, while the latter is denoted by $a \wedge b$, and is called the *join* of a and b. We are now ready to state the clock theorem.

Theorem 4. *Let U be a universe equipped with two fixed adjacent stars, and let $\mathcal{S}$ denote the set of all states on U with this choice of stars. Then $\mathcal{S}$ has a unique clocked state and a unique counterclocked state, and any state in $\mathcal{S}$ can be reached from the clocked state via a sequence of clockwise moves. Similarly any state can be reached from the counterclocked state via a series of counterclockwise moves.*
Define the partial order $\leq$ on $\mathcal{S}$ by declaring that $S \leq S'$, if and only if there exists a sequence of counterclockwise moves connecting S to S'. Then the partially ordered set $(\mathcal{S}, \leq)$ is a lattice, whose largest element is the clocked state, and whose smallest element is the counterclocked state.

Proof. The proof of the clock theorem is rather long, and has been omitted from this thesis. The interested reader may consult [8]. □

To remedy the lack of proof, we provide instead the comforting figure 3.17, which illustrates the lattice structure of $\mathcal{S}$ for a particular universe. As usual, the lattice is drawn in the form of a Hasse[3] diagram, in which a line segment that goes *upwards* from a state S_1 to state S_2 signifies that $S_1 < S_2$ (meaning that $S_1 \leq S_2$, and $S_1 \neq S_2$). For each state of this figure, we illustrate which clockwise moves are necessary to go from the particular state to states below.

[3] Helmut Hasse: 1898 - 1979, Germany

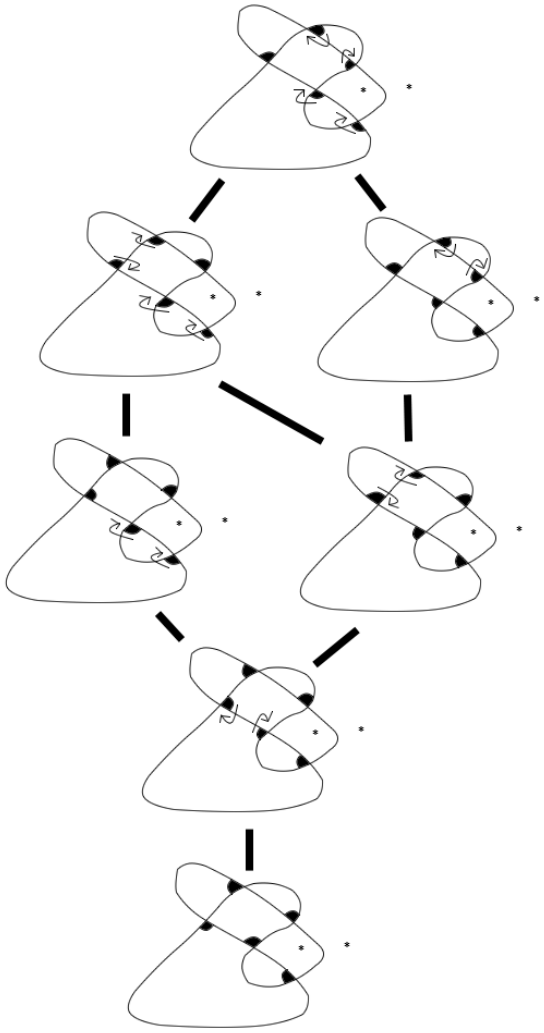

Figure 3.17: The lattice structure for a particular universe, and for a given choice of fixed stars.

3.3 State polynomials

We introduce here the state polynomial, which will turn out to be crucial at the climax of proving that $\chi_c(L) = \chi(L)$ for alternative links L. At first, the state polynomial will be defined only, when a given choice of fixed adjacent stars of a universe are given, but we will soon see that the polynomial turns out to be independent of the choice of stars. Let U be an oriented universe, and suppose some vertex has been given a state marker. The state marker is, by definition, categorized as either a black hole, a white hole, an up state or a down state, depending on what corner of the vertex, the state marker has been positioned in. The exact categorization is shown in figure 3.18.

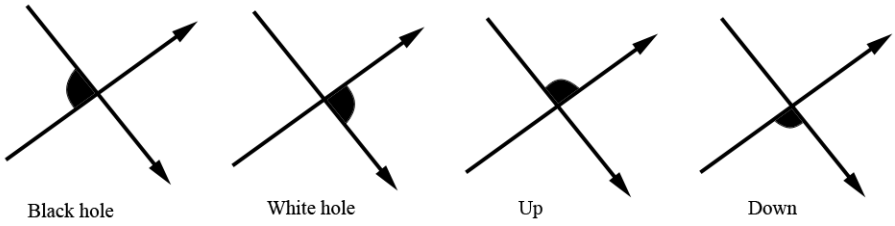

Figure 3.18: Classification of state markers.

As for this choice of terminology, neither [7] nor [8] offer an explanation, and the reader should feel free to make up his or her own.

Definition 9. *Let S be a state of an oriented universe U. Let b denote the number of black holes of S. The* sign $\sigma(S)$ *of S is given by*

$$\sigma(S) = (-1)^b.$$

Let U be an oriented universe, and numerate the vertices of U as $V_1, \ldots, V_n$. Suppose that each of the four corners of each of the vertices of U has been given a *label*, as illustrated in figure 3.19.

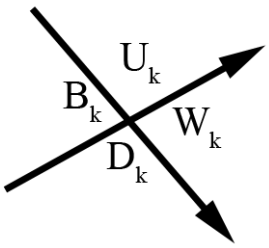

Figure 3.19: Labels of the corners of vertex V_k.

Thus each vertex V_k has been given four labels W_k, D_k, B_k, U_k, where each label has been affiliated with a specific corner of the vertex. A universe with labels at each vertex will be called a *labeled universe*, and will usually be denoted by K.
Let S be a state of the universe U. We wish to define a so-called *inner product* $\langle K|S\rangle$, which exploits the labels of U, and which will lead to the definition of the state polynomial. One is not to be confused by our "inner product" into thinking of the usual vector space inner products. In fact, we have no vector space structure whatsoever.

Definition 10. *Let K be a labeling of an oriented universe U, and let S be a state of U. The inner product $\langle K|S\rangle$ is defined as follows:*

$$\langle K|S\rangle = \sigma(S)V_1(S)V_2(S)\cdots V_n(S) \in \mathbb{Z}[W_1, D_1, B_1, U_1, \ldots, W_n, D_n, B_n, U_n],$$

where $\sigma(S)$ is the sign of the state S, and where $V_i(S)$ denotes the label touched by the state marker of S at the i'th vertex, i.e. $V_i(S)$ is W_i, D_i, B_i or U_i depending on the position of the label at the vertex V_i, with the exception that $V_i(S)$ denotes $W_i + B_i$ if the state marker touches either W_i or B_i, and if the two corners belong to the same region, and similarly for $D_i + U_i$.

Definition 11 (State polynomial)**.** *Let U be an oriented universe, and let two adjacent stars be given. Denote by $\mathcal{S}$ the set of all states on U with this given choice of stars, and let K denote the labeled universe with underlying oriented universe U. The* state polynomial *$\langle K|\mathcal{S}\rangle$ is then given by:*

$$\langle K|\mathcal{S}\rangle = \sum_{S\in\mathcal{S}} \langle K|S\rangle \in \mathbb{Z}[W_1, D_1, B_1, U_1, \ldots, W_n, D_n, B_n, U_n].$$

The state polynomial will most likely seem like a strange thing to consider at this point, but the reader may take comfort in the fact that a certain simplified form (taken modulo suitable things) will turn out to be a link invariant, and more importantly, it will be the main tool in considerations on maximal Euler characteristic.

3.3.1 Permutation assignments

Let U be an oriented universe, whose regions have been numbered as $R_1, R_2, \ldots, R_n, R_{n+1}, R_{n+2}$, where the last two regions are chosen to be adjacent. Let $\mathcal{S}$ be the set of states of U with stars in the last two regions R_{n+1} and R_{n+2}. The universe U has n vertices, and a given state of U corresponds to a (unique) assignment of regions $R_1, R_2, \ldots, R_n$ to vertices. Choose an indexing of the vertices such that the assignment $R_i \mapsto V_i$ (for $i = 1, 2, \ldots, n$) corresponds to a state S_0 of $\mathcal{S}$ of sign $+1$, i.e. $\sigma(S_0) = +1$.
Let S_n denote the symmetric group on n letters $1, 2, \ldots, n$, and for a permutation $p \in S_n$, denote by $\mathrm{sgn}(p)$ its sign, i.e. $\mathrm{sgn}(p)$ is equal to $(-1)^s$, where s denotes the number of transpositions (2-cycles) in any decomposition of p into transpositions.

Definition 12. *A* permutation assignment *for $\mathcal{S}$ is a function*

$$P\colon \mathcal{S} \to S_n,$$

given as follows: For a state $S \in \mathcal{S}$, the permutation $P(S)$ is given on a number $i \in \{1, 2, \ldots, n\}$ by $P(S)(i) = j$, where j is the number such that V_j has its state marker in region R_i.

For example, it is clear that $P(S_0) = \mathrm{id}$, where id denotes the identity permutation.

Lemma 3. *Let $S' \in \mathcal{S}$ be a state obtained from $S \in \mathcal{S}$ via just one state transposition, and let $P\colon \mathcal{S} \to S_n$ be a permutation assignment. Then*

$$sgn(P(S')) = -sgn(P(S)).$$

Proof. Denote by V_i and V_j the vertices, whose state markers switch regions. Say, in S the state marker of the vertex V_i is in the region R_{k_i} and the state marker of V_j is in R_{k_j}, while in S' these two state markers have switched regions. Suppose $m \neq k_i, k_j$. Since the vertex that has its state marker in region m is the same for both S and S', we certainly have that $P(S)(m) = P(S')(m)$. By definition, we also have that

$$P(S)(k_i) = i, \text{ and } P(S')(k_i) = j,$$
$$P(S)(k_j) = j, \text{ and } P(S')(k_j) = i.$$

In conclusion, $P(S') = P(S)(k_i\ k_j)$, where $(k_i\ k_j)$ is a transposition. The result follows. □

This lemma combined with the next one provides a sign consistency of sorts between the states of a universe and the corresponding permutations under a permutation assignment.

Lemma 4. *Let $S' \in \mathcal{S}$ be a state obtained from $S \in \mathcal{S}$ via just one state transposition. Then $\sigma(S') = -\sigma(S)$.*

Proof. The proof goes by considering all possible positions of black and white holes in the two relevant regions. For example, consider figure 3.20, in which the left state marker is a white hole of S, while the right state marker is a black hole. After the state transposition, the left marker is of down type, while the right marker is of up type. Thus, the parity of the number of black holes has changed, as was to be proved. A similar argument of course applies, if the state markers had been switched the other way around, i.e. if they were originally of down and up type, and were switched to become a black and a white hole.

Figure 3.20: A state transposition changes the state sign.

Figure 3.21 shows the remaining three cases, where the labels W and B represent possible black and white holes. Considering this figure completes the proof.

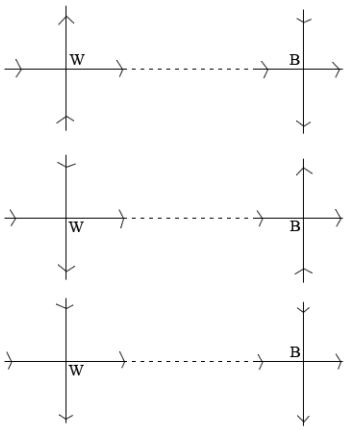

Figure 3.21: The three remaining constellations.

□

As promised, the two recent lemmas combine to show the following sign consistency between a state and the permutation corresponding to that state under a permutation assignment.

Proposition 2. *Let $P\colon \mathcal{S} \to S_n$ be a permutation assignment. Then $\sigma(S) = sgn(P(S))$ for all $S \in \mathcal{S}$.*

Proof. As we have already remarked, we have $P(S_0) = \mathrm{id}$, the identity permutation, and by definition $\sigma(S_0) = 1 = \mathrm{sgn}(\mathrm{id})$. Let S be an arbitrary state in $\mathcal{S}$. According to the clock theorem, S is obtained from S_0 via some sequence of state transpositions. Take any such sequence, and denote by t its number of state transpositions. Then by lemma 3, we have $\mathrm{sgn}(P(S)) = (-1)^t \mathrm{sgn}(P(S_0)) = (-1)^t$, but by lemma 4 we have also that $\sigma(S) = (-1)^t \sigma(S_0) = (-1)^t$, completing the proof. □

3.3.2 The Alexander matrix

We show now that the state polynomial is actually the determinant of a certain matrix. As before, let $R_1, R_2, \ldots, R_n, R_{n+1}, R_{n+2}$ be an ordering of regions of a given oriented universe U, such that the stars of U are contained in the regions R_{n+1} and R_{n+2}. Choose an ordering $V_1, \ldots, V_n$ of the vertices giving rise to a permutation assignment. Assume that U is labeled as in figure 3.19.

Definition 13. *The* Alexander matrix $A(K) = [A_{ij}]$ *of the labeled universe K is the $n \times (n+2)$ matrix with rows corresponding to the ordered set of vertices, and with columns corresponding to the ordered set of regions, and with entries defined as follows:*

$$A_{ij} = \begin{cases} 0, & R_j \text{ does not touch } V_i, \\ B_i,\ W_i,\ U_i \text{ or } D_i, & R_j \text{ touches } V_i \text{ in the corner corresponding to this label}, \\ B_i + W_i \text{ or } U_i + D_i, & R_j \text{ touches two corners at the vertex } V_i. \end{cases}$$

By "a region touching a vertex" we mean of course that the vertex is a point at the boundary of that region.
Letting again $\mathcal{S}$ denote the set of states on U with the given choice of stars, we denote by $A(K, \mathcal{S})$ the $n \times n$ matrix obtained from $A(K)$ by deleting the last two columns R_{n+1} and R_{n+2}. The square matrix $A(K, \mathcal{S})$ is called the *reduced* Alexander matrix.

Proposition 3. *The state polynomial is the determinant of the reduced Alexander matrix, i.e.*

$$\langle K|\mathcal{S}\rangle = \det A(K, \mathcal{S}).$$

Proof. Recall the definition of the determinant:

$$\det A(K, \mathcal{S}) = \sum_{p \in S_n} \operatorname{sgn}(p) A_{p(1)1} A_{p(2)2} \cdots A_{p(n)n},$$

where A_{ij} denotes the (i, j)-entry of $A(K, \mathcal{S})$. We argue that each non-zero term in the determinant expansion is also a term of the state polynomial, and vice versa.
Let $p \in S_n$ be some permutation. The term corresponding to this p is non-zero, if and only if it is true for all i that the region R_i touches the vertex with index $p(i)$. Take such a non-zero term. We want to find a state $S \in \mathcal{S}$, such that $\langle K|S\rangle = \pm A_{p(1)1} A_{p(2)2} \cdots A_{p(n)n}$. At the vertex with index $p(i)$, we position a state marker in region R_i. We can do this, as R_i touches $V_{p(i)}$. As permutations are bijections, all vertices will receive a state marker, and no region will contain two state markers: We have a state S. The following argument shows why S has the desired property. Suppose that region R_i touches the vertex of index $p(i)$ in the corner with label L_i, so that $A_{p(i)i} = L_i$. Then as the vertex $V_{p(i)}$ has been equipped with a state marker in region R_i, this state marker must fall on the label L_i, so that L_i is a factor of $\langle K|S\rangle$. This argument works for all i, and would have worked just as well, if R_i had incidentally touched $V_{p(i)}$ in two corners instead of one. We are left to check that the sign is correct, but this is where the chosen permutation assignment P comes in. We have in fact $P(S) = p$. Indeed, if $p(i) = j$, then vertex number j has its state marker in region i, but this is the exact meaning of $P(S)(i) = j$. Thus $\sigma(S) = \operatorname{sgn}(P(S)) = \operatorname{sgn}(p)$. This argument can be reversed to see that for any state, there is a permutation $p \in S_n$ such that $\operatorname{sgn}(p) A_{p(1)1} \cdots A_{p(n)n} = \langle K|S\rangle$, thus completing the proof. □

3.4 Star independence

When applying the state polynomial to a universe with a general labeling, we can certainly not expect the polynomial to be independent of the choice of stars. However, when using specific labelings, the polynomial *will* turn out to be star independent, a fact on which we will rely heavily.

3.4.1 Independence using the standard labeling

We have introduced the state polynomial in a general setting, but we will now see the state polynomial for a specific and convenient labeling. In fact, we introduce the *standard label* for a universe, in which each corner of a vertex receives labels as shown in the left picture of figure 3.22. This labeling will be abbreviated as shown in the right picture of the same figure, so that blank corners represent the label "1". The way to think of the standard labeling is of course to think of the B-label as hovering over a potential black hole, and similarly for the W-label.

Figure 3.22: The standard label.

Using the standard labeling, the following proposition follows immediately from the definition of the state polynomial.

Proposition 4. *Let U be an oriented universe with a fixed choice of adjacent stars, and let K denote the standard labeling of U. As usual, let $\mathcal{S}$ denote the set of states on U. Then for all states $S \in \mathcal{S}$, we have $\langle K|S\rangle = (-1)^{b(S)}B^{b(S)}W^{w(S)}$, where $b(S)$ denotes the number of black holes in S, and $w(S)$ denotes the number of white holes in S. Consequently, we have*

$$\langle K|\mathcal{S}\rangle = \sum_{b,w}(-1)^b N(b,w,\mathcal{S})B^bW^w,$$

where $N(b,w,\mathcal{S})$ is the number of states in $\mathcal{S}$ with b black holes and w white holes.

We will see in a moment that the number $N(b,w,\mathcal{S})$ is in fact independent of the choice of fixed stars of U, and we way therefore denote it by $N(b,w)$. In [8], the following result is conjectured:

Duality Conjecture. *For all $r,s \geq 0$, we have $N(r,s) = N(s,r)$.*

The claim is thus that for any choice of fixed adjacent stars, the number of states with r black holes, and s white holes, is the same as the number of states with s black holes and r white holes. This conjecture was later proved in [5].
It will turn out to be useful to be able to attach a number to each region of a universe in a very specific manner.

Definition 14. *An* Alexander indexing *of a universe U is the assignment of an integer to each region of U such that adjacent regions have indices differing by one, as specified in figure 3.23 by the orientation of their common boundary.*

Figure 3.23: The rule for the increase or decrease of indices in an Alexander indexing.

Questioning the existence and usefulness of the Alexander indexing is justified. We immediately settle the existence, while postponing usefulness for later.

Lemma 5. *Every universe has an Alexander indexing.*

Proof. Split each vertex as if applying Seifert's algorithm. This gives rise to a finite collection of simple closed curves, which we will also refer to as Seifert circles. By considering the regions of U before the splittings took place, we see that regions that end up being part of the same Seifert circle should have the same Alexander index, see figure 3.24. It thus suffices to index each region in the diagram of Seifert circles in such a way that adjacent regions receive indices according to the rule of definition 14, but this can be done easily as follows: Choose the "unbounded" region (by which we mean the region containing the outside of the universe), and give it some index, say 0. Any Seifert circle adjacent to the unbounded region is then given an index as dictated by the indexing rule. Since Seifert circles are disjoint, only nested Seifert circles are adjacent, which is why no two Seifert circles sharing boundary with the unbounded region can be adjacent. In conclusion, any Seifert circle, which is adjacent to the unbounded region, receives an index of $+1$ or -1, and as no such Seifert circles are adjacent, this does not violate the definition of Alexander indexing. Consider then one of these Seifert circles C of index $+1$ or -1. There may be a bunch of Seifert circles inside of C, but these are indexed exactly as before, but now with C playing the part of the unbounded region. This proves the lemma. □

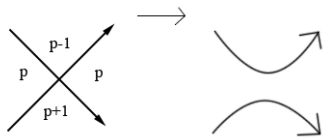

Figure 3.24: Regions that merge to become part of the same Seifert circle must have the same Alexander index.

In figure 3.25, we see the technique of the proof of lemma 5 in action. We are almost ready to begin the proof of our first result on star independence. We only need the following auxiliary lemma.

Lemma 6. *Let K be a labeled universe, with underlying universe U, and take some Alexander indexing of U. As the columns of the Alexander matrix $A(K)$ of K are in one-to-one correspondence*

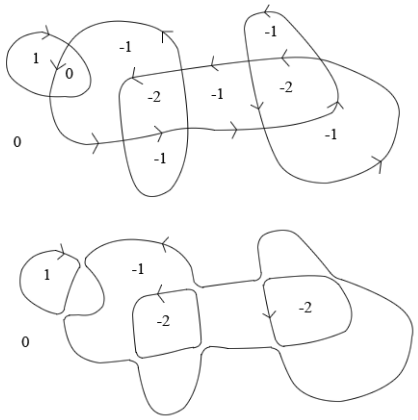

Figure 3.25: The technique of the proof of lemma 5 in action.

with the regions of U, we can speak of the columns of a specific index. Let C_p denote the sum of the columns of index p. Then if x is a solution to the quadratic equation $x^2 + x(B + W) + 1 = 0$, we have that

$$\sum_{p\in\mathbb{Z}} x^p C_p = 0.$$

Proof. Let x solve $x^2+x(B+W)+1 = 0$. Then for all $p \in \mathbb{Z}$, we have $x^{p+2}+Bx^{p+1}+Wx^{p+1}+x^p = 0$. To prove the lemma, we prove that any entry of the vector $\sum x^p C_p$ is of the form $x^{p+2} + Bx^{p+1} + Wx^{p+1} + x^p$. Without loss of generality consider the first row of $A(K)$. This row either has four non-zero entries 1, B, W, and 1, or it has three non-zero entries 1, $B + W$, and 1. We consider only the first case, as the second is similar. Among the two columns containing the 1's of row 1, take the one of lowest index p. Then the columns containing B and W are adjacent to the region of index p, and must both have indices $p+1$. The column containing the last 1 consequently has index $p + 2$, and the first entry of the vector $\sum x^p C_p$ is thus $x^p + Bx^{p+1} + Wx^{p+1} + x^{p+2}$, as we set out to prove. □

We can now prove our first result on star independence.

Theorem 5. *Let K be a standard labeling of an oriented universe U, and let $\mathcal{S}$ and $\mathcal{S}'$ be the sets of states on U for different choices of fixed adjacent stars. Then*

$$\langle K|\mathcal{S}\rangle = \langle K|\mathcal{S}'\rangle.$$

Using proposition 4, we thus obtain the star independence of $N(b, w) = N(b, w, \mathcal{S})$.

Proof. Write $\rho = B + W$, and denote by α and $\overline{\alpha}$ the roots of the polynomial $x^2 + \rho x + 1$. These roots then satisfy $\alpha\overline{\alpha} = 1$ and $\alpha + \overline{\alpha} = -\rho$. By lemma 6, we have thus

$$\sum_{p\in\mathbb{Z}} \alpha^p C_p = 0,$$

$$\sum_{p\in\mathbb{Z}} \overline{\alpha}^p C_p = 0.$$

Let k be some index. Multiply the first of these relations by $\overline{\alpha}^k$, and subtract the second multiplied by α^k. Upon letting $[\alpha] = \alpha - \alpha^{-1}$, we obtain

$$\begin{aligned}
0 &= \overline{\alpha}^k \sum_{p\in\mathbb{Z}} \alpha^p C_p - \alpha^k \sum_{p\in\mathbb{Z}} \overline{\alpha}^p C_p \\
&= \alpha^{-k} \sum_{p\in\mathbb{Z}} \alpha^p C_p - \alpha^k \sum_{p\in\mathbb{Z}} \alpha^{-p} C_p \\
&= \sum_{p\in\mathbb{Z}} \alpha^{p-k} C_p - \sum_{p\in\mathbb{Z}} \alpha^{k-p} C_p \\
&= \sum_{p\neq k} \left(\alpha^{p-k} - \alpha^{k-p}\right) C_p \\
&= \sum_{p\neq k} [\alpha^{p-k}] C_p. \qquad (3.1)
\end{aligned}$$

Let $A(K)$ be the Alexander matrix of K, the standard labeling of U. Let k, s be distinct numbers, for which there exist columns with these as indices, and denote by $A(k,s)$ the square matrix obtained by deleting from $A(K)$ a column of index k and a column of index s. Let $F(k,s) = \det A(k,s)$. We may assume that the last two columns, the ones corresponding to the regions R_{n+1} and R_{n+2}, have indices 1 and 0, respectively, and that $A(1,0)$ is the matrix obtained by deleting these two columns. Then by proposition 3, we have

$$\langle K|\mathcal{S}\rangle = F(1,0).$$

Let s, k, and r be three different indices. Notice that $[\alpha^{r-k}] = -[\alpha^{k-r}]$. Then (3.1) yields

$$[\alpha^{k-r}] C_r = \sum_{p\neq k,r} [\alpha^{p-k}] C_p. \qquad (3.2)$$

Letting $\equiv$ denote equality up to sign, we claim now that

$$[\alpha^{k-r}] F(k,s) \equiv [\alpha^{k-s}] F(k,r). \qquad (3.3)$$

To see this, consider first the left-hand-side, and bring the element $[\alpha^{k-r}]$ into the determinant $F(k,s)$ by multiplying it onto a column of index r. By (3.2), this column can be written as a linear combination of columns of index not equal to k. But each of these columns in this linear combination are already columns of the matrix $A(k,s)$, except of course for the particular column of index s that had been removed from $A(K)$ to form $A(k,s)$. Thus, when replacing the column of index r, multiplied by $[\alpha^{k-r}]$, by the linear combination in 3.2, the linearity of the determinant shows that $[\alpha^{k-r}]F(k,s)$ is equal (up to sign) to the determinant of the matrix obtained by replacing the column of index r by the column of index s, thus proving the claim.
Applying (3.3) to the triple (k,r,t), we get

$$[\alpha^{r-k}] F(r,t) \equiv [\alpha^{r-t}] F(r,k),$$

and combining this with (3.3) as it is, we see that

$$[\alpha^{r-t}] F(k,s) \equiv [\alpha^{k-s}] F(r,t).$$

In particular, we may choose indices such that $k - s = 1$ and $r - t = 1$, in which case we have

$$F(k, s) \equiv F(r, t).$$

But we already remarked that $\langle K|\mathcal{S}\rangle = F(1, 0)$, and since $\langle K|\mathcal{S}'\rangle \equiv \det A(r, t) = F(r, t)$ for some choice of columns, such that $r - t = 1$, we obtain

$$\langle K|\mathcal{S}\rangle \equiv \langle K|\mathcal{S}'\rangle.$$

Since the sign of a monomial coefficient of the form $B^b W^w$ in any of these polynomials is given intrinsically by $(-1)^b$, we have in fact equality. This completes the proof. □

3.4.2 Independence using link labelings

We are finally able to let links enter the picture. In the upcoming terminology, we will see that links are special cases of labeled universes, and as such, we can apply the state polynomial to them. Most importantly, the state polynomial will almost be a link invariant. In fact, it is so close to being an invariant that if we take it modulo a certain small polynomial, it *will* be an invariant.
Let L be a link, and let D be some projection of L. The difference between the diagram D and a universe is the extra piece of information at each crossing telling us which strand is above the other. We store this extra piece of information in a *labeled* universe by agreeing on the identifications of figure 3.26.

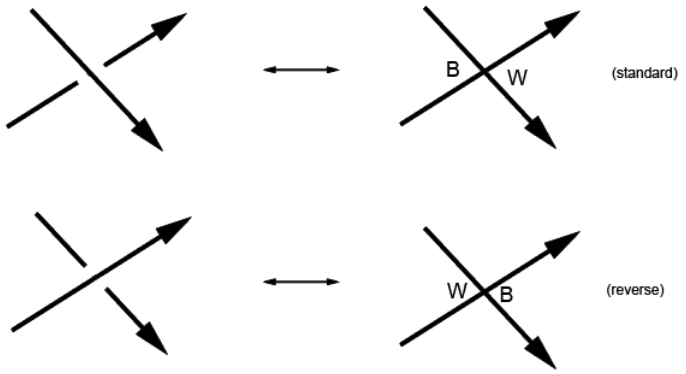

Figure 3.26: The code for bringing links into the language of universes.

Given a link L with a connected diagram D, the above encoding gives us a labeled universe. Choosing a pair of adjacent stars in the universe of D, it thus makes sense to apply the state polynomial to D. On grounds that will later be seen to be reasonable, we will confuse the diagram D with the link L, and when finding the state polynomial $\langle D|\mathcal{S}\rangle$, we will instead write $\langle L|\mathcal{S}\rangle$. For a given state S, the monomial $\langle L|S\rangle$ is thus $\sigma(S)B^x W^y$, where x, respectively y, denotes the number of coincidences

between state markers of S and B-labels, respectively W-labels. As suggested in the headline of this subsection, we have the following result.

Theorem 6. *Let K be a link with underlying universe U, and for a given choice of fixed adjacent stars, let $\mathcal{S}$ denote the set of states on U. Then the state polynomial $\langle K|\mathcal{S}\rangle$ is independent of the choice of stars, and we may denote it by $\langle K\rangle$. Furthermore, if K, $\overline{K}$, and L are links that differ at just one crossing as pictured in figure 3.27, then their polynomials are related by the exchange identity*

$$\langle K\rangle - \langle \overline{K}\rangle = (W - B)\langle L\rangle.$$

We will refer to this crossing as the critical crossing, and to the corresponding vertex of the universe underlying K and $\overline{K}$ as the critical vertex.

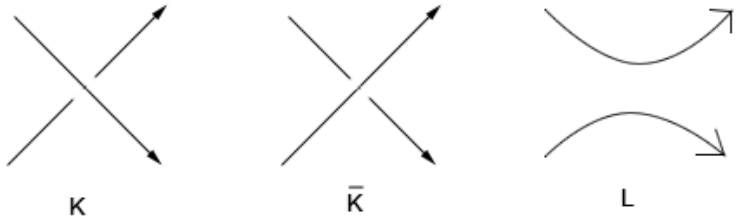

Figure 3.27: Three links that are the same except for in a small neighborhood of one crossing.

Proof. Recall that universes were defined to be connected. We will however allow ourselves to speak of a disconnected graph as a universe, keeping in mind all along that we are not very serious about it.

With the names of figure 3.27, it may certainly happen that the universe underlying L is not connected. We have not defined the state polynomial on such universes, but we argue why it is sensible to let $\langle L\rangle = 0$. We agree that the universe underlying K and $\overline{K}$ is U, and that the universe underlying L is U'. In case U' is disconnected, the appearances of K, $\overline{K}$, and L are as in figure 3.28, where the bottom black boxes contain the same in each of the three pictures, and similarly for the upper black box.

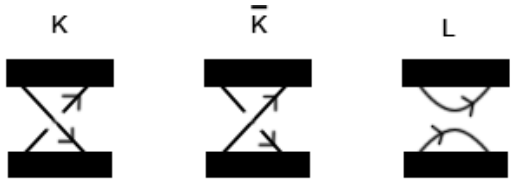

Figure 3.28: The universe underlying L is disconnected.

In this case, we cannot have a state marker of the form shown in figure 3.29.

Figure 3.29: Not a possible state marker.

Indeed, the two adjacent stars would have to be in either the bottom or the top black box, say the bottom one. The bottom and top black boxes are universes in their own right (with the arcs of L added), so in particular, the top black box must have state markers in all but two regions. It does not have a state marker in the "unbounded region", that is, the region outside of the black boxes, and as the two stars of U were positioned in the bottom black box, the upper black box has state markers in all other regions, a contradiction. In conclusion, the state marker of U at the vertex of figure 3.29 must be of type up or down, but then this state marker makes no contribution to the state polynomials of K and $\overline{K}$. As all other vertices of K and $\overline{K}$ have the same labelings, we have then $\langle K\rangle = \langle \overline{K}\rangle$, so that $\langle K\rangle - \langle \overline{K}\rangle = 0$, and we are justified in defining $\langle L\rangle = 0$. The assumption that U' is disconnected is equivalent to the assumption that the dotted line of figure 3.30 does not cleave a region of U'.

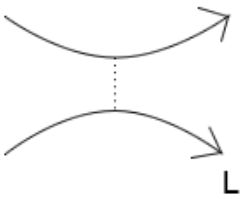

Figure 3.30: If the dotted line does not cleave a region of U', then $\langle L\rangle = 0$.

Assume now that this dotted line does cleave a region of U', so that the universe U' is connected. The universe U' inherits its stars from U, so denote by $\mathcal{S}'$ the set of states on U'. Suppose first that in U' a star is found in the same region as that of the dotted line. This star is inherited from U, and as such, it is naturally positioned on either to the left or to the right of the dotted line. Assume right, the other case being similar. Let S' be a state in $\mathcal{S}'$. A state in $\mathcal{S}$ can be constructed uniquely from S' as follows. The universe U' has a state marker at each vertex, and as each vertex of U' is also a vertex of U, we leave the state markers of U' untouched when transferring them to U. One vertex of U is left, and at this vertex, we can only choose to let the state marker be positioned to

the left, i.e. opposite of the star so that the state marker is a black hole. Then

$$\langle K|S\rangle = -B\langle L|S'\rangle$$
$$\langle \overline{K}|S\rangle = -W\langle L|S'\rangle,$$

whereas

$$\langle K|S\rangle - \langle \overline{K}|S\rangle = (W-B)\langle L|S'\rangle.$$

We are left to account for all states of $\mathcal{S}$ with an up or down state marker at the critical vertex. Let S be such a state. Then $\langle K|S\rangle - \langle \overline{K}|S\rangle = 0$, since the state marker at the critical vertex contributes a factor 1 to both $\langle K|S\rangle$ and $\langle \overline{K}|S\rangle$, and all other state markers contribute the same factors. Thus

$$\langle K|\mathcal{S}\rangle - \langle \overline{K}|\mathcal{S}\rangle = (W-B)\langle L|\mathcal{S}'\rangle.$$

Suppose next that the region that the dotted line of figure 3.30 cleaves does not contain a star. Let $\mathcal{L}$ denote the states of $\mathcal{S}'$ with a marker to the left of the dotted line, and let $\mathcal{R}$ denote the states with marker to the right of the dotted line, so that $\mathcal{S}' = \mathcal{L} \cup \mathcal{R}$. A state $\mathcal{L}$ corresponds to a state of $\mathcal{S}$ by closing the site at the dotted line, and filling in a state marker at the unoccupied site, and similarly for states in $\mathcal{R}$. Letting $\mathcal{W}$ denote the set of states of $\mathcal{S}$ with a white hole at the critical crossing, and letting $\mathcal{B}$ denote those with a black hole at that crossing, we have the correspondence of figure 3.31.

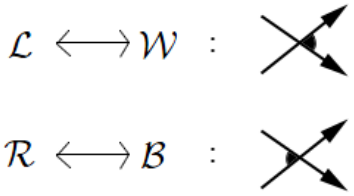

Figure 3.31: The correspondence between states of $\mathcal{S}'$ and a subset of states of $\mathcal{S}$.

Thus

$$\langle K|\mathcal{W}\rangle = W\langle L|\mathcal{L}\rangle,$$
$$\langle \overline{K}|\mathcal{W}\rangle = B\langle L|\mathcal{L}\rangle,$$
$$\langle K|\mathcal{B}\rangle = -B\langle L|\mathcal{R}\rangle,$$
$$\langle \overline{K}|\mathcal{B}\rangle = -W\langle L|\mathcal{R}\rangle,$$

and so

$$\langle K|\mathcal{W}\cup\mathcal{B}\rangle - \langle \overline{K}|\mathcal{W}\cup\mathcal{B}\rangle = (W-B)\langle L|\mathcal{L}\cup\mathcal{R}\rangle.$$

We are left to account for the states in $\mathcal{S}$, where the critical vertex has a state marker of type up or down, but we have already argued that for such states S, the difference $\langle K|S\rangle - \langle \overline{K}|S\rangle$ is 0, and so

$$\langle K\rangle - \langle \overline{K}\rangle = (W-B)\langle L\rangle.$$

This proves the exchange identity for an arbitrary choice of fixed adjacent stars. We use this identity to prove star independence by induction. An unknot diagram is a universe of zero crossings, and as this diagram has only two regions, there is just one choice of fixed adjacent stars. In general, as L has fewer crossings than K and $\overline{K}$, we may assume by induction that $\langle L \rangle$ is independent of the choice of stars. By the exchange identity, the polynomial $\langle K \rangle$ is independent, if and only if $\langle \overline{K} \rangle$ is independent. The links K and $\overline{K}$ are related by one crossing exchange. Any two links with the same underlying universe are related by a sequence of crossing exchanges, so it suffices to produce one link K', such that $\langle K' \rangle$ is independent of the star choice. For this purpose we let K' be the standard link, i.e. K' is the link on the universe underlying K with standard labelings at each vertex. Then proposition 4 shows that $\langle K' \rangle$ is independent of the choice of stars.

□

3.5 Topological invariance of the Conway polynomial

In the previous section, we saw that the state polynomial turned out to be independent of the choice of stars. By tweaking the state polynomial slightly, we can furthermore make it a topological link invariant. Let us recap quickly what it means for two links to be equivalent. For details, the reader may consult [3].

By definition, two oriented links L_1 and L_2 in S^3 are equivalent, if and only if they are ambient isotopic, or equivalently, if there is an orientation preserving homeomorphism $f\colon S^3 \to S^3$ with $f(L_1) = L_2$. Choose projections of L_1 and L_2 to some $S^2 \subset S^3$, and denote by D_1 and D_2 the resulting diagrams. It is a theorem that L_1 and L_2 are equivalent, if and only if their diagrams D_1 and D_2 are equivalent in the following sense: Two diagrams D_1 and D_2 are said to be equivalent, if they are related by a orientation-preserving homeomorphism of S^2 and by a sequence of Reidemeister moves, which are moves that alter the diagram locally, as pictured in figure 3.32, and leave the rest of the diagram untouched.

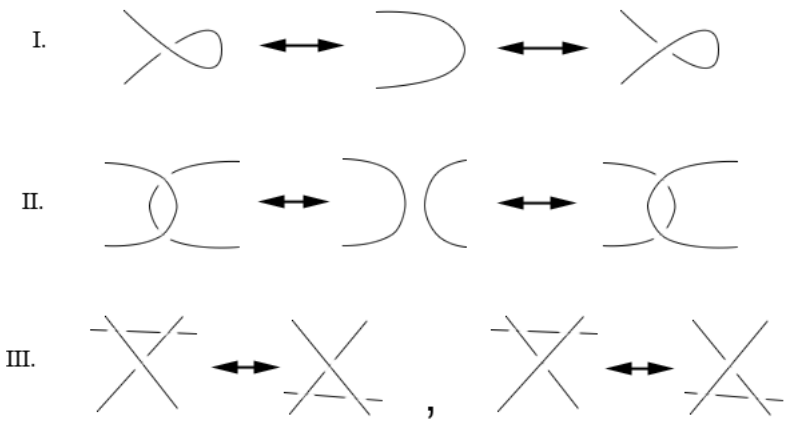

Figure 3.32: The three Reidemeister moves, also called the elementary moves.

We wish to investigate how the state polynomial reacts to equivalent diagrams. Notice first that if we perform an orientation-preserving homeomorphism on S^2, then the universe U underlying a diagram D is unchanged in the sense that the universe obtained after the homeomorphism is isomorphic to U as planar graphs. As such, the state polynomial of a link L is invariant under orientation-preserving homeomorphisms of S^2, and it suffices to consider the three Reidemeister moves.
Let K be a link. The state polynomial is an element of the polynomial ring $\mathbb{Z}[B, W]$. Let I be the ideal generated by the polynomial $BW - 1$, so that $\mathbb{Z}[B, W]/I$ is isomorphic to the ring $\mathbb{Z}[B, B^{-1}]$. Denote by $\psi\colon \mathbb{Z}[B, W] \to \mathbb{Z}[B, W]/I$ the quotient homomorphism.

Definition 15. *Let K be a link. The* Conway polynomial ∇_K *of K is defined by $\nabla_K = \psi\langle K\rangle$, where $\langle K\rangle$ is the state polynomial of K.*

As we will prove shortly, this is the desired modification of the state polynomial that ensures topological invariance. In fact, denoting topological equivalence by $\sim$ we have the following theorem.

Theorem 7. *Let $z = W - B$. Then*

1. *$K \sim K'$ implies $\nabla_K = \nabla_{K'}$,*

2. *$K \sim 0$ implies $\nabla_K = 1$ (where "0" denotes the unknot),*

3. *$\nabla_K - \nabla_{\overline{K}} = z\nabla_L$, when K, $\overline{K}$, and L are related as in figure 3.27.*

Proof. Part 1. We show first that equivalent links have identical Conway polynomials. Consider first moves of type I. As $\langle K\rangle$ is independent of star locations, we may assume that a star is *not* positioned

in the loop of the first part of figure 3.32. Then that region must contain a state marker, and we have then a one-to-one correspondence of states as shown in figure 3.33.

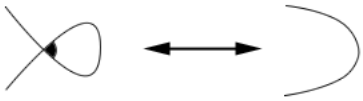

Figure 3.33: A one-to-one correspondence of states.

Depending on the orientation of the string, the state marker in the loop is either of type up or down, thus contributing an indifferent factor of 1 to the state polynomial. Thus $\langle K \rangle$ is invariant under moves of type I, and then likewise for ∇_K.
Next, consider moves of type II. For moves of this type, we have the two possible orientations of figure 3.34.

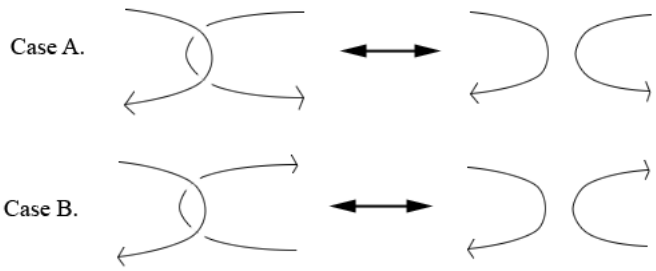

Figure 3.34: Possible orientations for moves of type II.

In case A, the crossing types are encoded as labels as shown in figure 3.35.

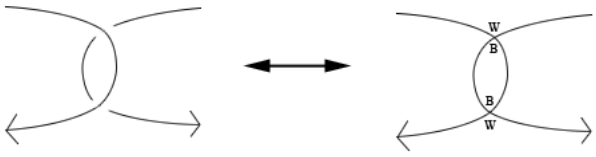

Figure 3.35: The encoding of crossings in case A.

Again, as the polynomial $\langle K \rangle$ is independent of the choice of stars, we may choose these as we wish. Let the stars be located as pictured in figure 3.36, where we also show the three possible placements of the state markers at the two visible vertices.

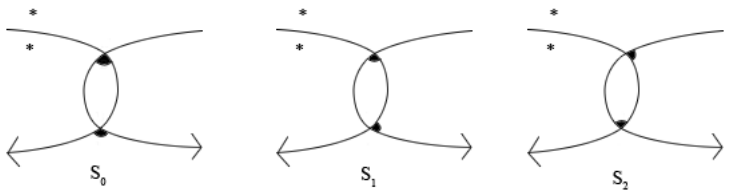

Figure 3.36: The three possible cases, when the stars have been chosen as shown.

For these diagrams, we may assume that the region above and below the the diagrams are distinct. Because otherwise there are no states of type S_0, and as S_1 and S_2 contribute equally, but with opposite sign, to the state polynomial, we have that the state polynomial of this universe is 0. But in this case, the "universe" obtained after applying the move of type II is disconnected, in which case its state polynomial is 0, by definition. See figure 3.37.

Figure 3.37: When the regions above and below the diagram coincides.

So assume that the regions X and Y are distinct. Then we have a one-to-one correspondence of states as pictured in figure 3.38.

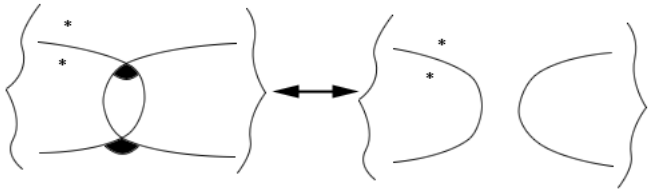

Figure 3.38: A one-to-one correspondence of states.

Again, S_1 and S_2 contribute equally, but with opposite sign, and hence only states of the form in the left-hand-side of figure 3.38 contribute to the state polynomial. Thus we have the state polynomial identity of figure 3.39.

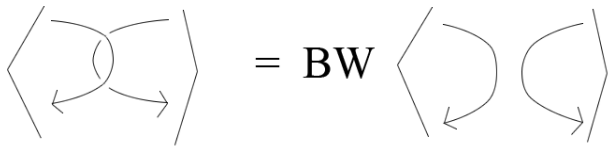

Figure 3.39: A state polynomial identity in case A.

Passing to the Conway polynomial, we have $BW = 1$ as needed. In case B, we have the encoding in figure 3.40.

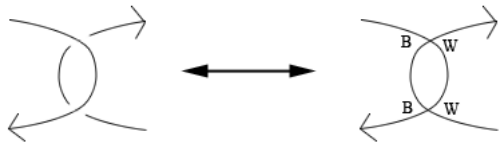

Figure 3.40: The encoding of the link in case B.

States of type S_1 and S_2 cancel each other's contributions again, and we are left to deal with S_0. However, according to the one-to-one correspondence above, in figure 3.38, it follows in this case that the state polynomial is invariant under moves of type II (and then so is the Conway polynomial). For moves of type III, we may again choose adjacent stars as we wish. In particular, we choose the stars in the regions shown in the left-hand-side of figure 3.41. After the move, we get the right-hand-side picture.

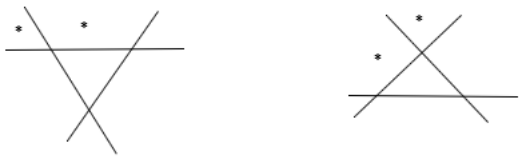

Figure 3.41: Performing the Reidemeister move of type III in the universe setting.

The moves of type III will be treated case by case. This is tedious, but to exhibit commitment, we handle one case. For instance, let S be the state pictured in figure 3.42, where the symbols $\otimes$ are placed in regions that do not have state markers at the triangle.

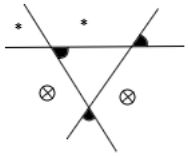

Figure 3.42: A state S in the setting of moves of type III.

When we do the move of type III, in which we move the horizontal line downwards below the central crossing, we get three possible states S'_0, S'_1, S'_2, as shown in figure 3.43.

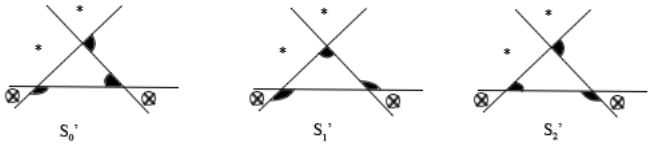

Figure 3.43: When S is changed by a type III move, three possible types of states occur.

We wish to keep track of the contributions from each one of these states to the state polynomial. Again, there are multiple cases for the appearance of the given link L, so we take a specific example. Suppose that K and K' are given locally by the diagrams shown in figure 3.44, in which we also show the corresponding encodings as labeled universes.

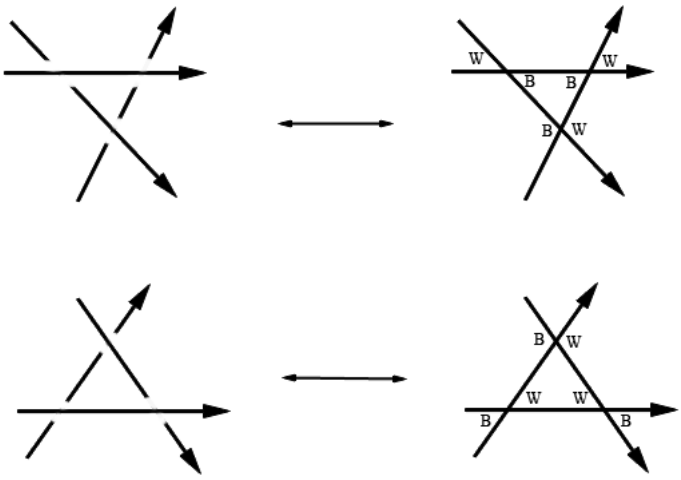

Figure 3.44: The encoding of a link before and after the move of type III.

Let α denote the contribution to the state polynomial $\langle K|S\rangle$ outside of the triangle. Then

$$\langle K|S\rangle = BW\alpha.$$

Also, by comparing figure 3.43 and figure 3.44, we see that

$$\langle K'|S_0'\rangle = -W^2\alpha,$$
$$\langle K'|S_1'\rangle = \alpha,$$
$$\langle K'|S_2'\rangle = W^2\alpha.$$

We thus have

$$\langle K'|S_0' \cup S_1' \cup S_2'\rangle = \alpha,$$

this polynomial being the sum of the three individual polynomials above it. In conclusion, we have $\nabla_K = \nabla_{K'}$. The remaining triangle states to be checked are listed in figure 3.45.

Part 2. By convention, we set $\nabla_0 = 1$, where 0 is the unknot. This is consistent with part 1, because if K is equivalent to the unknot, then K is certainly also equivalent to the knot of the left-hand-side of figure 3.46. When choosing stars as in the right-hand-side of that figure, there is only one possible choice for the state marker at the vertex, and this state marker falls at a 1. Hence $\nabla_K = 1$, as required.

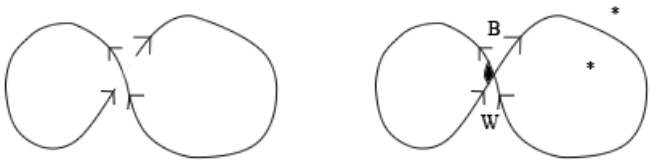

Figure 3.46: A knot equivalent to the unknot.

Part 3. This part was proved in theorem 6. □

3.6 Axiomatic Conway polynomial

The Conway polynomial, as described in the previous section, can in fact be shown to be a polynomial in the variable $z = W - B$ alone. What is even more interesting is that the properties proven about the Conway polynomial suffice for performing calculations. We will not go through the details, but refer instead to [8, chapter 5]. However, we do provide the axioms for completeness, and give a computational example.

Axioms for the Conway polynomial.

1. For each oriented knot or link K, there is an associated polynomial $\nabla_K(z) \in \mathbb{Z}[z]$, such that equivalent links receive identical polynomials.

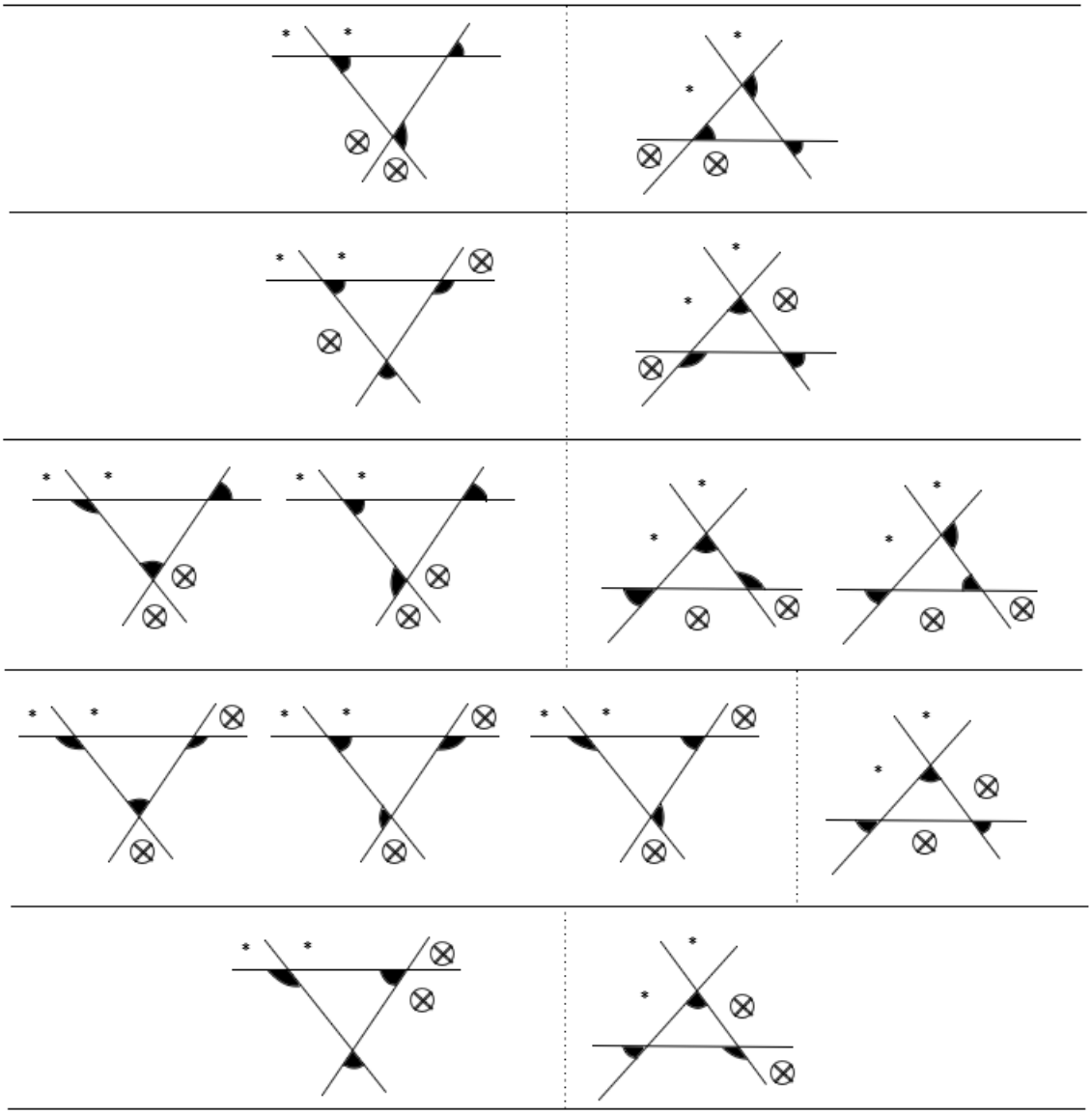

Figure 3.45: The remaining possible states at the triangle in a move of type III.

2. If K is the unknot, then $\nabla_K = 1$.
3. If K, $\overline{K}$, and L are three links that differ at one crossing as indicated in figure 3.27, then the corresponding polynomials are related by

$$\nabla_K - \nabla_{\overline{K}} = z\nabla_L.$$

We have already provided a polynomial that satisfies these three axioms, namely the state polynomial modulo the ideal $(BW - 1)$. The axioms are thus mutually consistent. However, we do not know if the axioms uniquely defines a polynomial invariant, but this is also the case. We refer again to [8, chapter 5]. To see the axioms in action, let us do a couple of examples.

Example 1. *For a split link L, we show that $\nabla_L = 0$. As L is split, it has a diagram of the form shown below in figure 3.47.*

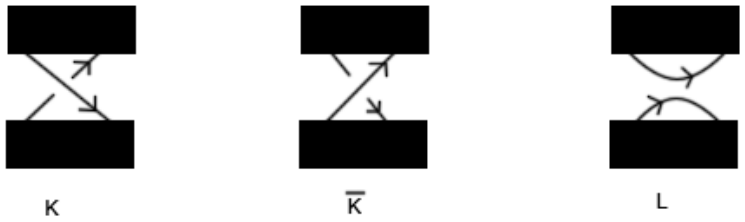

Figure 3.47: The most-right link L is split.

The link K is equivalent to the link $\overline{K}$, as letting the lower part of K undergo a 2π rotation yields $\overline{K}$. By axiom 1, we have $\nabla_K = \nabla_{\overline{K}}$. But by axiom 3, we have also $\nabla_K - \nabla_{\overline{K}} = z\nabla_L$, whereas $\nabla_L = 0$.

This example is important in concrete polynomial calculations, as we will see now.

Example 2. *We calculate ∇_K, where K is the trefoil knot. Change one crossing as shown in the first row of figure 3.48, so that K, $\overline{K}$, and L are related as in figure 3.27. Then by axiom 3, we have $\nabla_K = \nabla_{\overline{K}} + z\nabla_L$, and as $\overline{K}$ is the unknot, we obtain by axiom 2 that $\nabla_K = 1 + z\nabla_L$. The second row of figure 3.48 shows L, and the two knots obtained by changing one crossing of L in the two different ways. Hence $\nabla_L = \nabla_{\overline{L}} + z\nabla_U$, and as $\overline{L}$ is a split link, and as U is the unknot, we obtain $\nabla_L = 0 + z = z$, hence $\nabla_K = 1 + z\nabla_L = 1 + z^2$.*

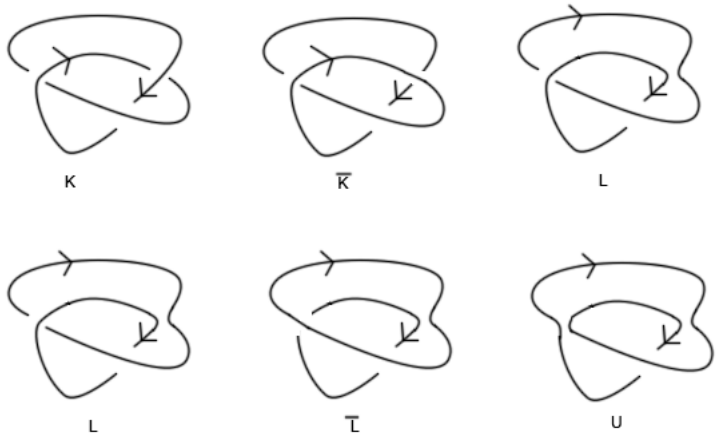

Figure 3.48: Axiomatic calculation for ∇_K of the trefoil knot.

It is a perhaps not altogether obvious fact that when calculating ∇_L for some link L, the calculation always reduces to knowing ∇_K for K the unknot or unlinks of $n > 1$ components. This is a consequence of the fact that given a knot, there is some sequence of crossing exchanges (changing crossings from over/under to under/over, or vice versa) that unknots the knot – and similarly for links.

3.7 Seifert's inequality

We want to find the Euler characteristic of a surface constructed by Seifert's algorithm. Let L be a link with projection D, which we will assume to be connected, and let U be the underlying universe. When running the first part of Seifert's algorithm, thereby making a collection of disjoint discs, each edge of U may be considered to be part of the boundary of one of these discs, leaving room along the disc boundaries only for the twisted bands. As we insert twisted bands to complete the Seifert surface, we insert a band for each vertex of U. The Seifert surface thus consists of one twisted band for each vertex of U, of one edge along the boundary for each edge of U, and of one open disc for each Seifert circle in the surface. Notice that twisted bands have the homotopy type of a point, so that the combined Euler characteristic of the Seifert surface is $V - E + S$, where V is the number of vertices of U, where E is the number of edges of U, and where S denotes the number of Seifert circles of the Seifert surface.

Reminder 1. *Recall that if S is a connected, orientable, compact surface with at least one boundary component, then*

$$\chi(S) = 1 - \rho(S),$$

where ρ is the rank of the first homology group of S, and where $\chi(S)$ as usual is the Euler characteristic.

Lemma 7. *Let K be a link (diagram) with underlying universe U, and let F be the Seifert surface for K obtained by applying Seifert's algorithm. Then*

$$\chi(F) = S(U) - R(U) + 2,$$
$$\rho(F) = R(U) - S(U) - 1,$$

where $S(U)$ is the number of Seifert circles obtained, and $R(U)$ is the number of regions of U.

Notice that $\chi(F)$ and $\rho(F)$ depends only on the underlying universe U.

Proof. Denote by $V = V(U)$ the number of vertices of U, and by $E = E(U)$ the number of edges of U. Let also $R = R(U)$ and $S = S(U)$. The 2-sphere has Euler characteristic 2, so

$$V - E + R = 2. \tag{3.4}$$

By the remarks preceding the lemma, we have that $\chi(F) = V - E + S$, and upon combining this with (3.4), we obtain the first part of the lemma. By reminder 1, we obtain the second part. □

Recall that to form a Jordan trail on a universe U, we split crossings and form *sites*. For an oriented universe, we distinguish between two kinds of sites. A site as on the left of 3.49 is called an *active* site, while the site to the right is a *passive* site. When we take an active site and changes it into a passive site, or vice versa, we speak of *reassembling* the site.

Figure 3.49: To the left, an active site. To the right, a passive site.

Recall that for a Jordan trail corresponding to a given state, we split vertices according to the position of the state marker at that vertex. Thus the black and white holes of a state are in one-to-one correspondence with the active sites of the corresponding trail.
We are about to find an upper bound on the degree of the Conway polynomial $\nabla_K(z)$. We think of $\nabla_K(z)$ as the state polynomial, so that $\nabla_K(z) = \langle K|\mathcal{S}\rangle$ with the identifications $BW = 1$ and $z = B - W$. The degree of $\nabla_K(z)$ is thus the maximal power of B in the state polynomial $\langle K|\mathcal{S}\rangle$, reduced by the relation $BW = 1$. As black and white holes of a state correspond exactly to the active sites of a trail, and as a state marker representing a black or white hole always falls on a B or a W when using the link labeling for the link K, the maximal power of B in ∇_K can be at most the largest number of active sites possible for a Jordan trail on the universe underlying K.

Lemma 8. *Let U be a universe with R regions and S Seifert circles. Any trail on U has at most $R - S - 1$ active sites.*

Proof. Start out by splitting every vertex of U to form active sites. This gives rise to the collection $\mathcal{C}$ of Seifert circles corresponding to U – by assumption there are S of these. Converting the set of Seifert circles $\mathcal{C}$ into a Jordan trail on U takes at least $S-1$ reassemblies, whence there are at least $S-1$ passive sites. Hence there are at most $V-(S-1)$ active sites, and as $V=R+2$, we obtain the desired result. □

By the remarks preceding the lemma, the content of the lemma thus implies that the maximal B-degree of $\nabla_K(z)$ is at most $R-S-1$.
The next result is a very easy consequence of the foregoing. It is however the very essence of the concluding part of this chapter, as explained after the proof of the theorem.

Theorem 8. *Let K be a link (diagram) with underlying (connected) universe U, and let F be the Seifert surface obtained by applying Seifert's algorithm to K. If $\rho = rank(H_1(F))$, then*

$$\deg \nabla_K(z) \leq \rho.$$

Proof. By lemma 8 (and the following remark), we have that $\deg \nabla_K(z) \leq R-S-1$. By lemma 7, we see that the right-hand-side of this inequality is exactly ρ, completing the proof. □

Recall that the Conway polynomial is a link invariant, and recall also that $\chi(F) = 1-\rho$. Thus, if we should hit upon a link diagram K for which $\deg \nabla_K = \rho$, we know that the given Seifert surface (constructed via Seifert's algorithm) has minimal genus among all other Seifert surfaces spanning links equivalent to K.

3.8 Defining alternative links

For a given diagram of an oriented link, we wish to adopt different conventions for labeling crossings according to their type. In figure 3.50, we see four different ways of labeling a crossing. The first is the well-known, and visually appealing, convention of letting one strand go under the other to signify the relative position of the corresponding strands of the link in space. The second is the so-called *dot convention*, in which two dots are placed to the left of the undercrossing strand, one dot on each side of the other strand. The third is the so-called *site-marking* convention. In this method of labeling, the crossing has been split to form a site, the splitting having been made in the only manner possible to be consistent with orientations, and to indicate that a crossing has been removed, the site has been drawn with cusps pointing to one another at where the crossing previously were. As in the dot convention, one dot has been placed to the left of the undercrossing strand, and we always position it in the opening of the site. Finally, we have already seen the fourth convention, known as *label-coding*. The letters B and W are placed opposite each other at the crossing, with the B placed in the position of the single dot in the site-marking convention, i.e. the B being placed such that the undercrossing strand has B to its left.

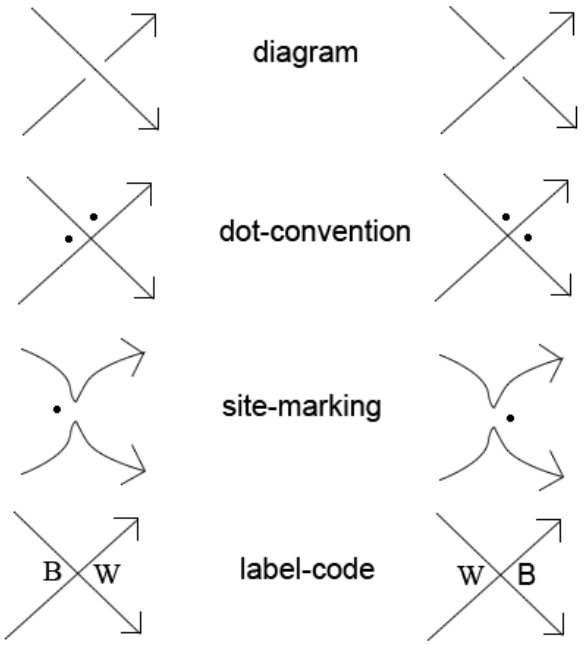

Figure 3.50: The different ways of encoding a crossing.

Most of these labeling conventions may seem rather mysterious, not to mention the strangeness of introducing four different such conventions instead of settling for just one. This is not madness. In a moment, we will make good use of these convention, and we will see the usefulness of each one of them. For now, we invoke only the dot and site-marking conventions to define alternative links. Let L be a connected oriented link diagram, labeled according to the dot-convention. As can be seen from figure 3.51, decorating the link diagram according to the site-marking convention gives rise to *the diagram of Seifert circles* for the link, with dots at each site. Letting CL denote the set of Seifert circles obtained from the diagram L, we can thus also speak of labeling the diagram CL according to the site-marking convention. In fact, whenever we speak of labeling the diagram of Seifert circles, we shall mean labeling it according to the site-marking convention, so that we from this diagram easily can see what the original link diagram looked like.

Definition 16. *A link diagram L divides the plane into a finite number of connected sets, called* regions*, and similarly, the set CL of Seifert circles divides the plane into a finite set of connected components, called* spaces *of CL.*

By dint of this definition, we can thus speak of two markings of the diagram CL as being in the same space. We now introduce alternative knots.

Definition 17. *Let L be a connected, oriented link diagram, and label the diagram CL of Seifert circles of L according to the site-marking convention. We say that the link diagram L is* alternative*, if for all spaces of CL, any two markings in that space are of the same type.*

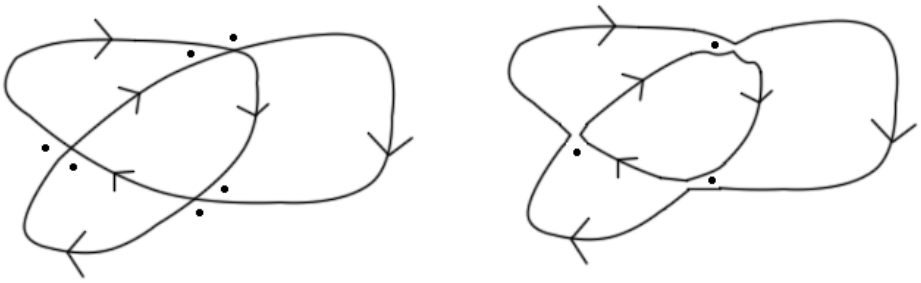

Figure 3.51: The trefoil knot with dot labels and with site labels.

In other words, given any space of CL, all marks in that space are either of the type indicated on the left-hand-side of figure 3.50, or otherwise they are all of the type indicated on the right-hand-side of that figure. We see thus from the right-hand picture of figure 3.51 that the given trefoil knot diagram is alternative. As was the case for alternating links, we agree that whenever a given link has some alternative link diagram, that link will be called alternative.
It will be a convenient visual aid to make a checkerboard coloring of a given link diagram, so that diagonally adjacent regions receive the same color. When passing to the diagram of Seifert circles, each space in this diagram receives a solid color. For example, see figure 3.52.

Definition 18. *When checkerboard coloring a connected link diagram K, spaces of the diagram CK of Seifert circles that receive the same color are said to have the same* parity.

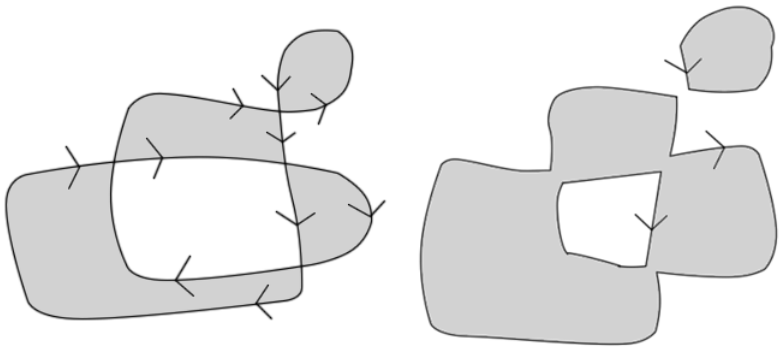

Figure 3.52: Each space in the diagram of Seifert circles receives the same solid color.

We will argue very shortly that alternating links are alternative. There do exist alternative links, which are not alternating, the smallest example of which is the $(3,4)$-torus knot, shown in figure 3.53. This knot has been catalogued as 8_{19} in the knot tables. It is apparent from the left-hand picture of this figure that the chosen projection is not alternating, and we see from the right-hand picture that the knot *is* alternative.

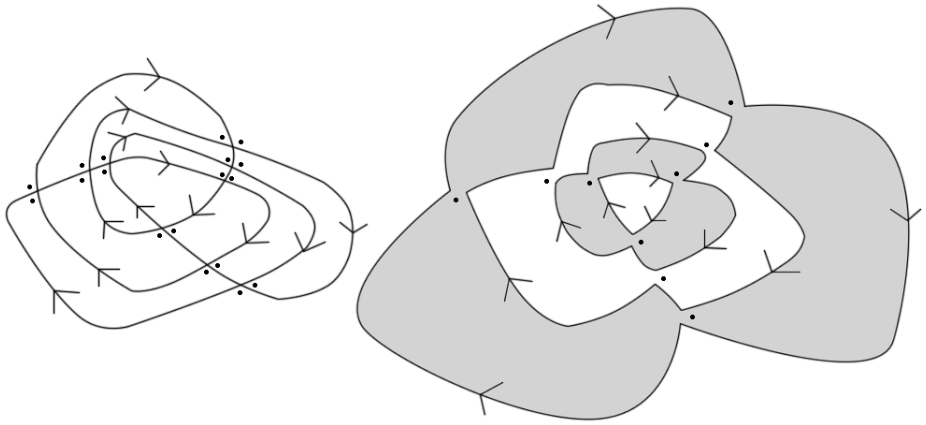

Figure 3.53: The $(3, 4)$-torus knot and its Seifert circle diagram.

Lemma 9. *An alternating link diagram is alternative.*

We skip the formal proof. Consider instead figure 3.54, the upper part of which shows the two possible local situations of an alternating diagram. The lower part is the translation of these local pictures into Seifert surface diagrams. We see that for the first alternating weave, the diagram of Seifert circles appears to have markings of different types in spaces of opposite parity. The second alternating weave translates to a diagram of Seifert circles, in which the markings end up in the same space, and where the markings are of the same type, as they should be for an alternative link.

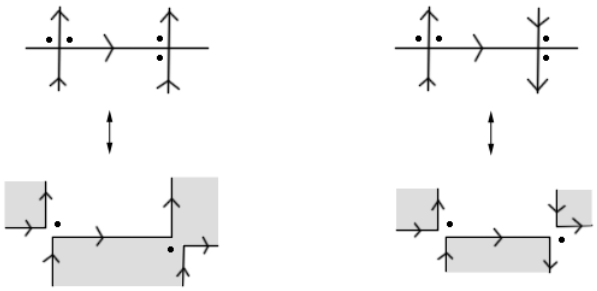

Figure 3.54: Translating the local picture of alternating links to diagrams of Seifert circles.

Remark 1. *There is a more accurate result on alternating links as follows. A link diagram is alternating, if and only if it is alternative and spaces in the diagram of Seifert circles receive the same or different marking type according to whether they have the same or different parity. Figure 3.54 testifies to this.*

3.9 The Alternative Tree Algorithm

We are finally prepared to take on the goal of this thesis.

Theorem 9. *Let L be a connected alternative link diagram, and let F_L be the surface obtained from applying Seifert's algorithm to L. Then F_L is a maximal Euler characteristic surface for the link represented by L. In fact, we have* $\deg \nabla_L = \rho(F_L)$.

We already argued that when $\deg \nabla_L = \rho(F_L)$, we do know that the surface F_L is of minimal genus, so it suffices to prove this part. The line of thought for this part is as follows. Notice from figure 3.50 that when the site-marking code and the label code are superimposed, then the dot always falls on the B. For states, this means that for every vertex with a state marker at the dot, this state marker contributes a B to the state polynomial. In the diagram CL of Seifert circles, we obtain a trail on the universe U underlying L by reassembling some of these sites, and the state polynomial of the corresponding state (recall the states-trails correspondence) reaches its maximal degree precisely when a minimum of sites have been reassembled (thus maintaining the maximal number of active sites), and when each state marker at an active sites falls on the dot, contributing a B to the state polynomial.
Let S_L denote the number of Seifert circles in CL. If on CL we reassemble $S_L - 1$ sites, then there remain $V - S_L + 1$ active sites, where V is the number of vertices of U. But Euler's theorem says that $V = R - 2$, so that $V - S_L + 1 = R - S_L - 1$, and according to lemma 7, this is exactly $\rho(F_L)$. Thus, if we can construct a trail on U by reassembling $S_L - 1$ sites in the diagram CL of Seifert circles, and if we in the corresponding state have that every state marker at an active site falls on a dot, then $\deg \nabla_L = \rho(F_L)$.
We describe an algorithm that constructs such trails, the so-called *Alternative Tree Algorithm* (ATA). In the diagram CL of Seifert circles, we referred to each connected part as a space of the diagram, while each connected part of the link diagram was called a region. The regions of L are visible in CL, because even though they are part of the same space of CL, they are being separated by sites.

Alternative Tree Algorithm.

Step 1. Let L be an alternative link projection, and denote by CL the diagram of Seifert circles of L decorated with site marking dots. Choose a pair of stars in adjacent regions of L.

Step 2. For each star, grow a tree in CL rooted at a star. A tree can branch from one region of L to another, if and only if the following three conditions are fulfilled:

a The second region is unoccupied by tree branches.

b There is a site opening from the first region to the second (site orientation unimportant).

c At an active site, the marking dot must be in the second region (site orientation unimportant).

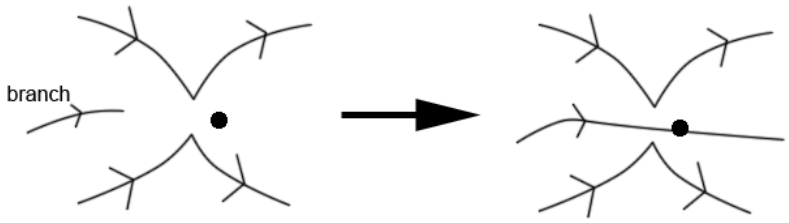

Figure 3.55: Growing a tree, letting it branch from one region to another.

Let the trees branch until **a**, **b**, and **c** can no longer be satisfied.

Step 3. There are active sites that open up to regions occupied by tree-branches, but which do not themselves have branches passing through them (as such branching violates part 2). These sites will be reassembled to form passive sites, thereby allowing new access for the trees. We indicate this reassembly by placing a circle around the site, as in figure 3.56. With this change, repeat step 2 and 3 until no further growth is possible, so that each site has a branch passing through it.

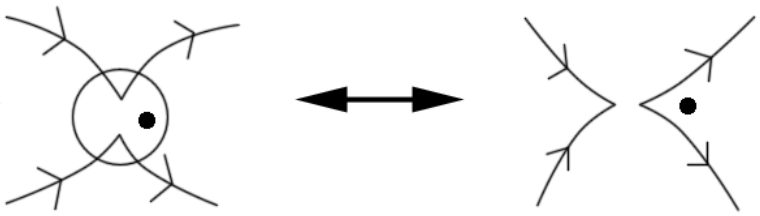

Figure 3.56: Changing an active to a passive site.

Step 4. Use the two trees to create a state S. In particular, if a tree grows from one region through a site to another region, then place a state marker in the second region (at the vertex corresponding to the site).

Before we argue why this algorithm does what it is supposed to, we ease understanding by providing examples. In figure 3.57, we see the figure-eight knot and its diagram of Seifert circles equipped with the site-marking dots.

Figure 3.57: The figure-eight knot, and its Seifert circles.

The process of applying the ATA to the above diagram is shown in figure 3.58. Notice also that in the left-hand-side of figure 3.59, we have a Jordan trail on the universe, and even better is that this Jordan trail was obtained by growing a tree rooted at each star, so that the corresponding positioning of state markers does give rise to a state.

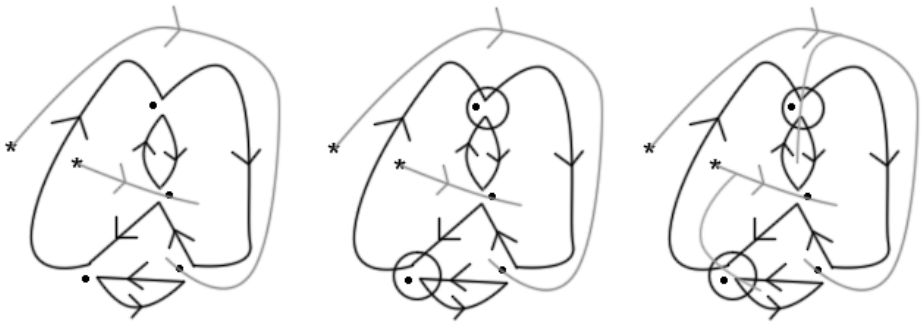

Figure 3.58: Running through the ATA with the figure-eight knot.

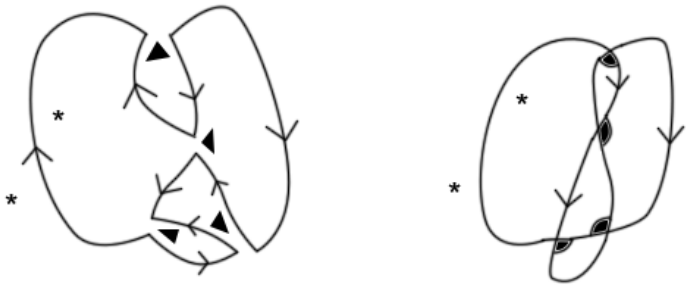

Figure 3.59: The state obtained from ATA on the figure-eight knot.

Yet another example, where we apply the ATA to the link diagram shown in figure 3.60. In figure

3.61, we see the result, which is now self-explanatory. In figure 3.62, we see another branching choice than that of figure 3.61. This testifies to the fact that the state constructed by the ATA is not unique. In fact, depending on the branching choices, the ATA produces a lot of states, and we are going to argue that it produces exactly all the maximal states.

Figure 3.60: A link and its corresponding Seifert circle diagram.

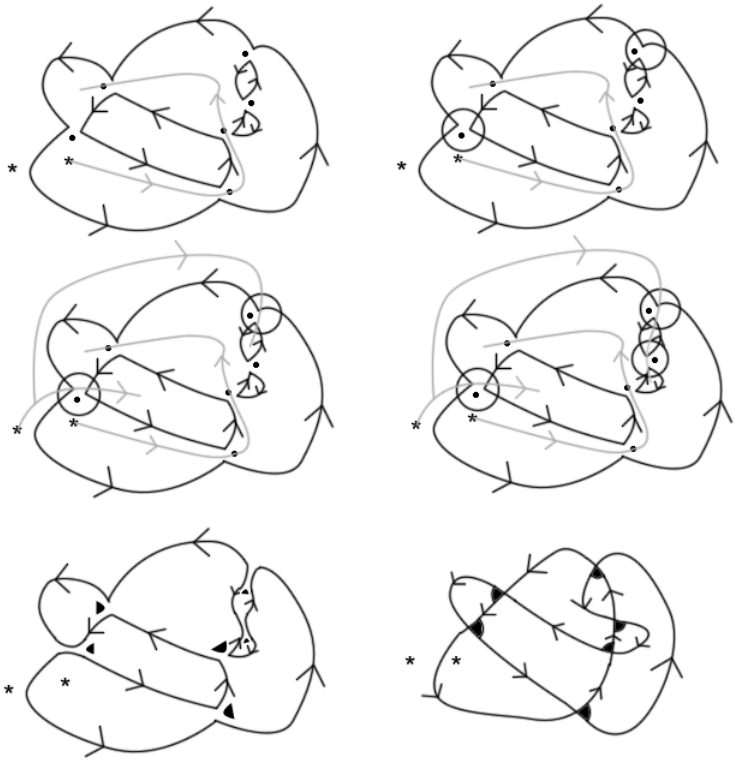

Figure 3.61: Applying ATA to a link.

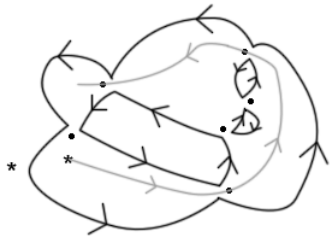

Figure 3.62: Another branching choice.

Assume for the moment that ATA does its job, thus producing all states with maximal B-powers. We have the following very pressing question: For instance, could ATA applied to some alternative link produce two maximal states, but where the states have opposite signs? Then the state polynomial would take on the appearance

$$+B^{\rho(F_L)} - B^{\rho(F_L)} + \text{lower degree terms},$$

and the contributions from the maximal states happen to cancel each other! For such a case, we would have $\deg \nabla_L < \rho(F_L)$. No sweat: This cannot occur, as we now observe.

Important observation 1. *If S and S' are states obtained by ATA from the same link diagram L, then S and S' have the same sign, i.e. $\sigma(S) = \sigma(S')$.*

The reason is that different branching choices of ATA always occur within the same space of CL. By definition, all markers in a given space are of the same type, and thus whichever branching choice we make leaves invariant the number of black and white holes in the resulting state.

In the case of the diagram of Seifert circles, we are interested in seeing how many reassemblies are necessary to form a Jordan trail on the corresponding universe. It will be helpful to consider this problem from a more general point of view, in which we consider an arbitrary collection of disjoint circles. For two given disjoint circles, we denote a reassembly by a straight line segment between them, as shown in figure 3.63.

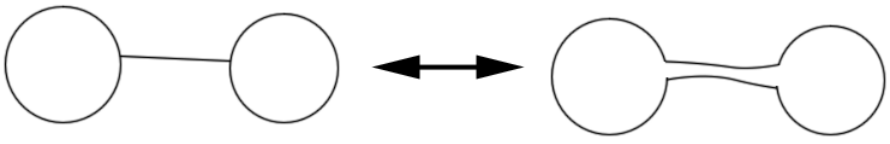

Figure 3.63: A line segment between two circles indicates a reassembly.

For just one circle, we need zero reassembly lines to form a Jordan trail. For a collection of $s > 1$ disjoint circles, we connect one circle to another by a straight line segment, so that this pair of circle melts into being just one circle. By induction, the new set of $s - 1$ circles can be transformed into a

Jordan trail by choosing $s-2$ reassemblies. Consequently, the original s circles can be transformed into a Jordan trail by choosing $s-1$ reassembly lines, see figure 3.64 for an example.

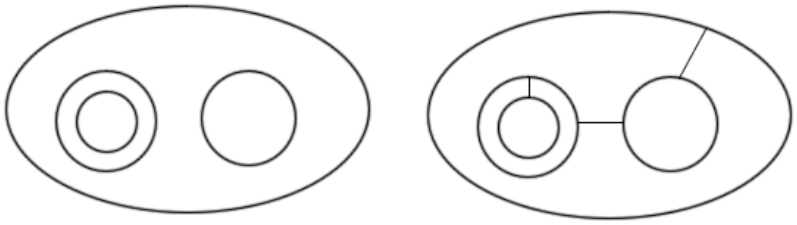

Figure 3.64: Choosing 3 reassemblies in a diagram of 4 circles.

The diagram CL of Seifert circles is of course a special case of this, and if S_L denotes the amount of Seifert circles, we need only S_L-1 reassemblies (i.e. changes from active to passive sites) to create a Jordan trail on the universe underlying L.
Returning to the general constellation of s circles in the plane, notice also that when we choose $s-1$ reassembly lines that turn the set of circles into a simple closed curve, each space remains connected. In fact, by choosing such $s-1$ reassembly lines, the spaces will not only remain connected, they will become discs, as can be seen from figure 3.65.

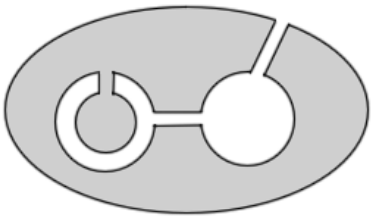

Figure 3.65: The spaces become disks.

Certainly, if the reassemblies are to produce a Jordan curve, this transformation of spaces into discs must occur. Conversely, to produce a Jordan curve with the least number of reassemblies, it suffices to choose a set of reassemblies in each space that cut that space to a disc. In terms of Seifert circles, we must choose S_L-1 reassemblies that cut each space to a disc, i.e. we must choose S_L-1 active sites to change into passive sites such that the spaces of the diagram are transformed into discs.
The following graph-theoretic lemma will show exactly why ATA can choose this set of reassemblies.

Definition 19. *A finite, connected, directed graph is said to be* even*, if each vertex touches an even number of edges, and if for each vertex, half the edges are outwardly directed, and half are inwardly directed.*

Given a graph G, a vertex v of G is said to be a *root* of a maximal tree in G, if v is contained in a maximal tree of G, and if every vertex of G can be reached from v by an outwardly oriented path in

the tree. Notice that an even graph cannot itself be a tree, because it can have no leaves.
The following graph-theoretic lemma is the key to the usefulness of the ATA.

Lemma 10. *Let G be an even graph, and let v be a vertex of G. Then v is the root of an oriented maximal tree T in G, where the orientation of T is induced by G.*

Proof. As noted, G is not a tree, and must therefore contain a cycle. As G is even, it also contains an oriented cycle A. Let $G' = G/A$, so that G' is the graph obtained from G by collapsing A to a point, i.e. G' is obtained from G by removing every edge of A, and by identifying all vertices in A to a single vertex. The graph G' still satisfies the conditions of the lemma. Indeed, for each vertex of the cycle A, we remove *two* incident edges, one which enters the vertex, and one which leaves it, thus maintaining an even number of edges incident to every vertex, and also maintaining the half-and-half condition.
By induction, we may assume that the lemma applies to G', where the vertex v may or may not be the vertex obtained by collapsing A to a point. Let T' be a maximal oriented tree in G', for which v is a root. In G', blow up the vertex corresponding to A, and extend the maximal tree T' to a maximal tree T in G, by extending T' along the cycle A. □

The lemma is applied as follows. Let L be an alternative link diagram, and let CL be the diagram of Seifert circles for L equipped with the site-marking convention. Let P denote a space of CL, and build a graph $G(P)$ on P as follows. The space P is divided into a number of regions separated by the sites of CL. For each region of P, we have a vertex of $G(P)$, and whenever two regions share a site (so that the regions are accessible to one another), there is an edge between the corresponding vertices of $G(P)$. This edge is directed towards the region containing the marking dot, see figure 3.66.

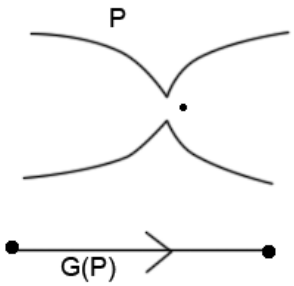

Figure 3.66: Constructing a graph on a space of CL.

The upshot is that the graph $G(P)$ is even – the Seifert circles are oriented coherently, and as all dots in a space P are of the same type (the link diagram being alternative), there is an even number of sites at each region, half of whose corresponding edge in $G(P)$ points towards the region, half of which point away, see figure 3.67.

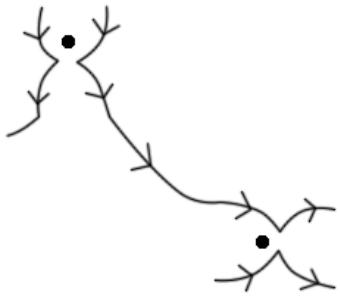

Figure 3.67: The graph $G(P)$ is even.

As $G(P)$ is even, we know that for whichever region of P that contains a star, lemma 10 ensures that we may grow an oriented maximal tree from this star, thus exactly meeting the conditions of growing a tree according to the rules of the ATA. As we have now grown a tree in P, the remaining active sites of that region are reassembled to passive sites, and these reassemblies exactly cut the given space into a disc. Doing this for each region, we obtain exactly a total number of $S_L - 1$ reassemblies, thus proving that the ATA actually terminates, and that it returns states of maximal B-powers. In conclusion, Seifert's algorithm applied to alternative diagrams do have maximal Euler characteristic.
Finally, we pose the question of pushing this theorem any further.

3.10 A possibly non-alternative link

A natural question to ask is: Do there exist non-alternative links with maximal Euler characteristic Seifert surfaces? If not, we have found the exact class of links L for which $\chi(L) = \chi_c(L)$. If there do exist other links, what are they?
Consider the knot diagram in figure 3.68. This knot diagram K is *not* alternative, but yet we can still apply the ATA to enumerate the high-power states of this knot. As it turns out, there are 11 states that contributes a term of the form $B^{\rho(L)}$ to the state polynomial, but among these 11 states, 7 have negative sign, while 4 have positive sign, leaving a coefficient of -3 on the high degree term of ∇_K.

Figure 3.68: A possibly non-alternative link.

It is unknown if there do exist a projection in which this diagram is alternative, a question which is seemingly very difficult to answer.

Bibliography

[1] Colin C. Adams. *The Knot Book.* American Mathematical Society, 2004.

[2] Glen E. Bredon. *Topology and Geometry.* Springer, 1993.

[3] Gerhard Burde and Heiner Zieschang. *Knots.* de Gruyter, 1985.

[4] David Gabai. *Genera of the Alternating Links.* Duke Mathematical Journal, vol. 53, no. 3, 677–681, 1986.

[5] Patrick M. Gilmer and Richard A. Litherland. *The Duality Conjecture in Formal Knot Theory.* Osaka Journal of Mathematics, vol. 23, 229–247, 1986.

[6] Rasmus Hedegaard. *Existence and Uniqueness of Knot Factorizations.* www.math.ku.dk/english/research/top/paststudents/heedegaard.MS-project.2009.pdf.

[7] Louis H. Kauffman. *Combinatorics and Knot Theory.* Contemporary Mathematics, Low Dimensional Topology, AMS, vol. 20, USA, 181–200, 1981.

[8] Louis H. Kauffman. *Formal Knot Theory.* Dover Publications, 2006.

[9] W.B. Raymond Lickorish. *An Introduction to Knot Theory.* Springer, 1997.